MARTIN MARIETTA ENERGY SYSTEMS LIBRARIES
3 4456 0351199 2

93

CENTRAL RESEARCH LIBRARY
DOCUMENT COLLECTION

ORNL-2841
UC-38 – Equipment, Methods, and Techniques
TID-4500 (15th ed.)

DESIGN, DEVELOPMENT, AND OPERATION OF METAL-DIAPHRAGM REACTOR-SERVICE PUMPS

E. C. Hise

CENTRAL RESEARCH LIBRARY
DOCUMENT COLLECTION
LIBRARY LOAN COPY
DO NOT TRANSFER TO ANOTHER PERSON
If you wish someone else to see this document, send in name with document and the library will arrange a loan.

OAK RIDGE NATIONAL LABORATORY
operated by
UNION CARBIDE CORPORATION
for the
U.S. ATOMIC ENERGY COMMISSION

Printed in USA. Price $2.00. Available from the

Office of Technical Services
Department of Commerce
Washington 25, D.C.

LEGAL NOTICE

This report was prepared as an account of Government sponsored work. Neither the United States, nor the Commission, nor any person acting on behalf of the Commission:

A. Makes any warranty or representation, expressed or implied, with respect to the accuracy, completeness, or usefulness of the information contained in this report, or that the use of any information, apparatus, method, or process disclosed in this report may not infringe privately owned rights; or

B. Assumes any liabilities with respect to the use of, or for damages resulting from the use of any information, apparatus, method, or process disclosed in this report.

As used in the above, "person acting on behalf of the Commission" includes any employee or contractor of the Commission, or employee of such contractor, to the extent that such employee or contractor of the Commission, or employee of such contractor prepares, disseminates, or provides access to, any information pursuant to his employment or contract with the Commission, or his employment with such contractor.

ORNL-2841
UC-38 – Equipment, Methods, and Techniques

Contract No. W-7405-eng-26

REACTOR EXPERIMENTAL ENGINEERING DIVISION

DESIGN, DEVELOPMENT, AND OPERATION OF METAL-DIAPHRAGM REACTOR-SERVICE PUMPS

E. C. Hise

DATE ISSUED

APR 26 1960

OAK RIDGE NATIONAL LABORATORY
Oak Ridge, Tennessee
operated by
UNION CARBIDE CORPORATION
for the
U. S. ATOMIC ENERGY COMMISSION

MARTIN MARIETTA ENERGY SYSTEMS LIBRARIES
3 4456 0351199 2

CONTENTS

Abstract 1

1. Introduction 1

2. General Description of Diaphragm Pumps 2

3. Diaphragm Heads 2

   3.1 Design of Diaphragms and Contour Plates 2

   3.2 Exclusion of Solids from Pump Cavity 32

   3.3 Seal Welding 33

   3.4 Pressure-Head Construction 35

4. Check Valves 39

   4.1 Configuration and Size 39

   4.2 Materials 40

   4.3 Containment 42

5. Operating History of Heads and Valves 42

6. Slurry Pumps 54

   6.1 Diaphragm Heads 54

   6.2 Check Valves 57

7. Drive Systems 58

   7.1 Pulse Generators 58

   7.2 Intermediate Barriers 62

   7.3 Phasing of Intermediate Systems 62

Acknowledgment 63

DESIGN, DEVELOPMENT, AND OPERATION OF METAL-DIAPHRAGM REACTOR-SERVICE PUMPS

E. C. Hise

ABSTRACT

Aqueous homogeneous reactors require pumps capable of injecting relatively small quantities of highly radioactive, corrosive fuel solution into the high-pressure system. These pumps must have a long maintenance-free life, be absolutely leak-proof, be resistant to the radioactive and corrosive environment, and be easily replaced by remote methods when necessary. Hydraulically driven metal-diaphragm pumps capable of meeting these requirements have been developed in the Homogeneous Reactor Project at ORNL. This report summarizes the development program, the operating experience with the pumps in tests and in reactor service, and the design information derived from the development program.

In this program, detailed information has been developed concerning drive systems, diaphragm heads, and check valves, the ultimate objective being the selection of a pumping unit on the basis of a sound knowledge of stresses, materials, configuration, and hydraulics. It has been shown that with proper design and materials selection, the diaphragm heads and check valves can operate continuously for about two years.

1. INTRODUCTION

In the course of development for the Homogeneous Reactor Project, and in operation of Homogeneous Reactor Experiment No. 1 (HRE-1) and the Homogeneous Reactor Test (HRE-2 or HRT), experience has been gained in the design and operation of metal-diaphragm pumps for feeding cool, corrosive, highly radioactive solutions and slurries into high-pressure circulating systems. The purpose of this report is to provide a manual based on past experience for the design, operation, and further development of pumps for this or similar service.

Specifically, pumps have been developed and operated

1. in the HRE-1
   (*a*) to deliver 0 to 1 gpm of radioactive UO_2SO_4 solution in H_2O against a 1000-psi head,
   (*b*) to deliver 0 to 1 gph of essentially pure D_2O against a 1000-psi head;
2. in the HRE-2
   (*a*) to deliver 0 to 1.5 gpm of radioactive UO_2SO_4 solution in D_2O containing additional D_2SO_4 at 100°F against a 2000-psi head,
   (*b*) to deliver 0 to 0.35 gpm of D_2O against a 2000-psi head;
3. for subsequent reactors – to deliver 0 to 10 gpm of radioactive ThO_2 slurry or UO_2SO_4 solution in H_2O or D_2O against a 2000-psi head.

These services have in common the requirements of controlled flow rate, no external leakage of process fluid, predictable life of at least one year of continuous operation, and the possibility of simple, remote replacement of the process parts of the pumping systems. The following

discussion is intended to provide a basis on which metal-diaphragm pumps can be designed to meet a wide range of operating conditions, for reactor service or for use in other systems having parallel requirements.

2. GENERAL DESCRIPTION OF DIAPHRAGM PUMPS

The pumps described in this report are illustrated in Figs. 1 and 2. They consist of five main components: a diaphragm head, two check-valve assemblies, an intermediate barrier, and a pulse generator. Pulses produced by the pulse generator are transmitted by an oil system through the intermediate barrier to an intermediate water system, which in turn transmits the pulses to the process fluid in the diaphragm heads. Pulsations in the process fluid are converted to net flow by means of the inlet and outlet check-valve assemblies. In the reactor systems for which diaphragm pumps have been supplied, the process end – the diaphragm head and the check-valve assemblies – has been located within the reactor cell; the intermediate-system pipe passes through the shield; and the remainder of the intermediate system and all the pulse generating system are accessible outside the shield. A method for replacing the process head and check-valve assemblies is provided by placing them in a standardized cart, which is equipped with three connecting flanges. The flanges mate with three permanent flanges in the reactor cell, and the flange bolts extend through the cell wall so that they can be connected and disconnected from the outside. The arrangement is shown in Fig. 3.

3. DIAPHRAGM HEADS

3.1 Design of Diaphragms and Contour Plates

The metal diaphragm is the portion of the head which is most susceptible to failure, and therefore the design of the diaphragm and of those parts directly affecting its life is of primary concern.

The maximum deflection and the contour assumed by the diaphragm are controlled by the shape of the backup plate or contour plate which is provided to limit the stresses in the diaphragm by controlling the deflection. The basic design problem is to design a contour which provides a maximum volumetric displacement at a given maximum diaphragm stress. Limited experimental data indicate in general that if other factors are carefully controlled the measured stresses agree closely with the theoretical predictions based on the shape of the contour plate.

Although investigations of a variety of contours – including conical with a flat diaphragm and corrugated[1] with a corrugated diaphragm – have been reported in the literature, the two combinations of contour and diaphragm which have received the most attention, both by commercial pump manufacturers and at this laboratory, are the so-called "free-deflection" contour and the two-radii contour with flat diaphragms.

---

[1]W. A. Wildhock, R. F. Dressler, and E. C. Lloyd, *Trans. Am. Soc. Mech. Engrs.* 79, 65 (1957).

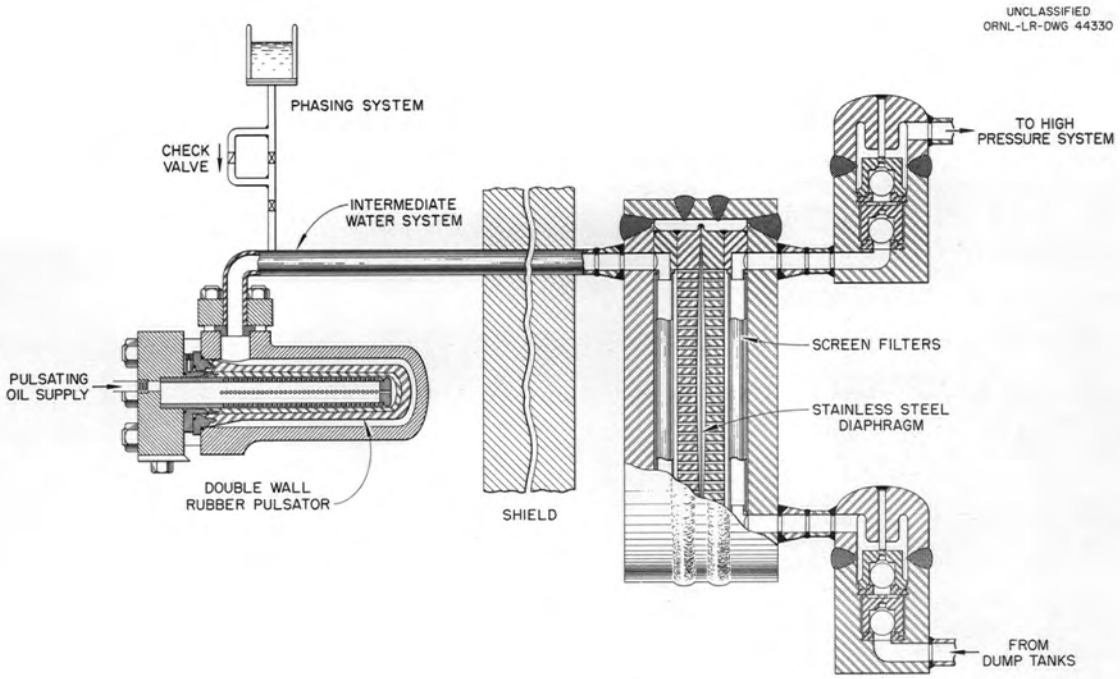

Fig. 1. Metal-Diaphragm Reactor Pump System.

Fig. 2. Unassembled Diaphragm Pump Head.

UNCLASSIFIED
PHOTO 42949

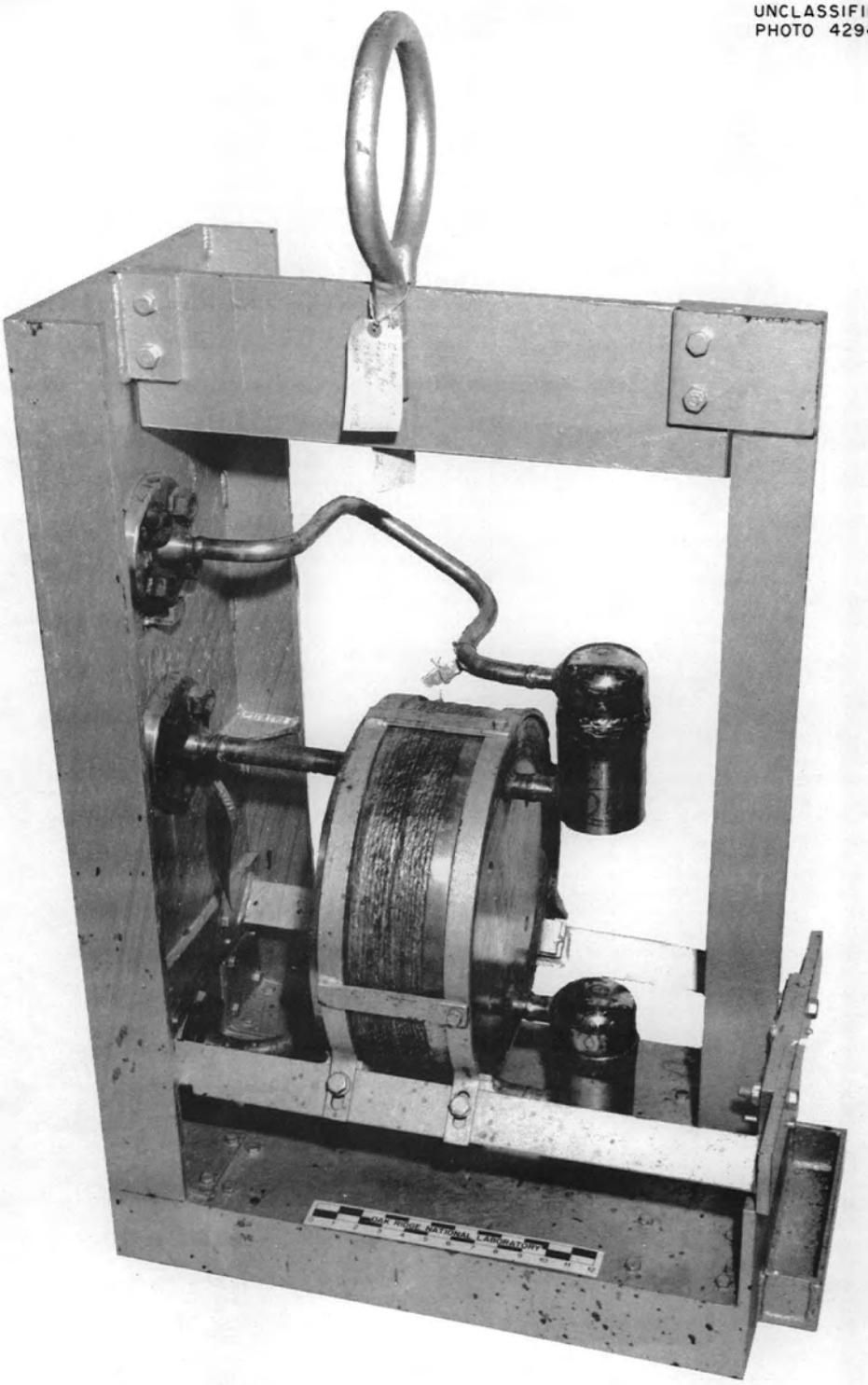

Fig. 3. Pump Head Assembly Ready for Installation in the HRT.

3.1.1 The Free-Deflection Contour. – The classical definition of a free-deflection contour is the contour which a circular, flat diaphragm with clamped edges and no other restraint will assume when subjected to a uniform pressure differential which is insufficient to cause stresses in the diaphragm in excess of the elastic limit. In current practice, however, the term "free-deflection contour" is applied to the figure of rotation of the curve which conforms to the simple relationship

$$Y = \frac{Y_0}{R^4}(R^2 - x^2)^2 \ , \tag{1}$$

where

Y = depth of the recess at x, the distance from the center line,

Y_0 = depth of the recess at the center line,

R = radius of the recess.

A cross-sectional view of such a contour is shown in Fig. 4.

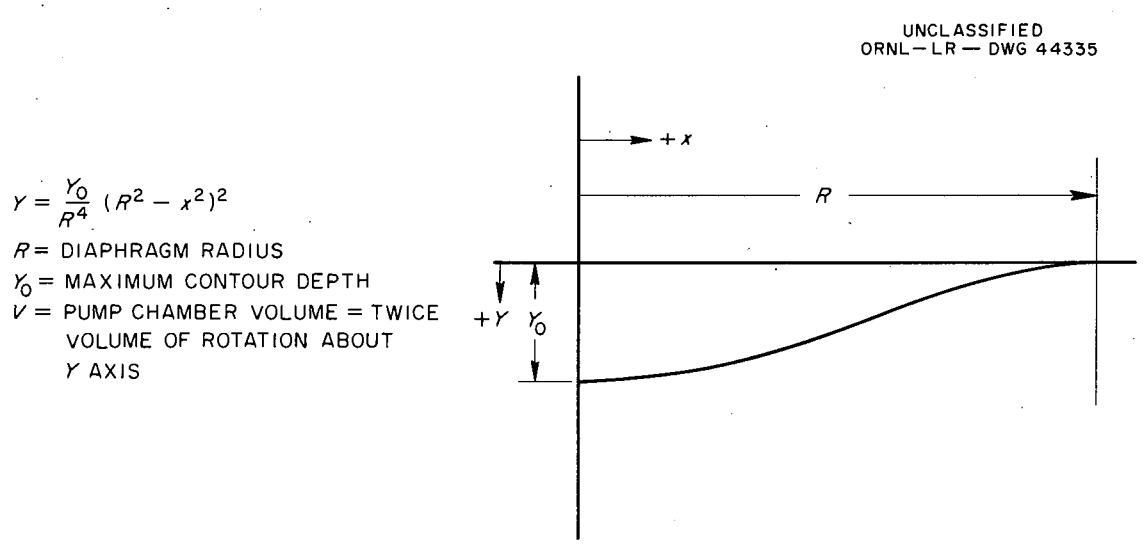

Fig. 4. Description of Free-Deflection Contour.

Equation (1) describes the contour predicted theoretically for a uniformly loaded circular diaphragm with clamped edges when bending stresses alone are considered.[2] Such a condition is approached as Y_0 approaches zero. A more accurate description for the contour in true free deflection can be evolved from an equation given by Timoshenko[3] which takes into account the

[2] S. Timoshenko, *Theory of Plates and Shells*, p 59–61, McGraw-Hill, New York, 1940.

[3] *Ibid.*, p 81, Eq. (h).

shear stresses in the diaphragm:

$$Y = \frac{Y_0}{R^4}(R^2 - x^2)^2 \frac{R^2(1-\nu)(R^2 - x^2) + 4b^2R^2}{R^2(1-\nu)(R^2 - x^2) + 4b^2(R^2 - x^2)} , \tag{2}$$

where b is the diaphragm thickness and ν is Poisson's ratio.

Way[4] has developed an even more accurate method of predicting the deflection, taking into account also the membrane stress in the diaphragm. (Timoshenko discusses Way's method in ref 5.) Way has tabulated stresses for 19 cases and shown excellent agreement with experimental data to within the limit of his calculation. However, the limit of Way's considerations is Y_0/b of about 1.4, while usually deflections Y_0/b of 3 to 20 are used in diaphragm pumps. It is seen from an examination of Eqs. (1) and (2) that the curve described by Eq. (1) has a longer radius of curvature at and near the clamped edge than the curve described by Eq. (2). A diaphragm forced to deflect in conformance with Eq. (1) will have a more uniform distribution of bending stress along a radius than a diaphragm permitted to deflect in accordance with Eq. (2). A linear extrapolation of Way's results (ref 4, Fig. 7) indicates that a diaphragm freely deflected to Y_0/b equal to 2.0 will have a radial bending stress of 36,000 psi at the edge. It therefore becomes apparent that a diaphragm permitted a true free deflection in the range of Y_0/b useful in diaphragm pumps would be stressed beyond its elastic limit.

The following equations developed by Pasqua[6] show that diaphragms deflected to the so-called "free-deflection" contour of Eq. (1) have a fairly uniform distribution of the radial principal stress and that useful deflections and volumetric displacements can be obtained with diaphragm stresses below the endurance limit of the material.

The total volumetric displacement, V, of a diaphragm moving from $+Y_0$ to $-Y_0$ between two "free-deflection" contour plates is given by

$$V = \frac{2\pi Y_0 R^2}{3} . \tag{3}$$

The radial membrane stress σ_{rm} is

$$\sigma_{rm} = E\left(\frac{Y_0}{R}\right)^2 \left[\frac{2}{3}\left(\frac{x}{R}\right)^4 - \left(\frac{x}{R}\right)^2 - \frac{1}{6}\left(\frac{x}{R}\right)^6 + 0.9762\right] , \tag{4}$$

where E is the modulus of elasticity of the diaphragm material.

The radial bending stress σ_{rb} is

$$\sigma_{rb} = \frac{2EbY_0}{(1-\nu)^2 xR}\left[3.3\left(\frac{x}{R}\right)^3 - 1.3\frac{x}{R}\right] . \tag{5}$$

---

[4]S. Way, *Trans. Am. Soc. Mech. Engrs.* 56, 627–36 (1934).

[5]Timoshenko, *op cit.*, p 338–42.

[6]P. F. Pasqua, notes dated June 26, 1958.

Figures 5, 6, and 7 are three families of curves showing the stroke volume, V, vs the diaphragm radius, R, at maximum radial principal stress levels ($\sigma = |\sigma_{rm}| + |\sigma_{rb}|$) of 15,000, 20,000, 25,000, 30,000, 35,000, and 40,000 psi for stainless steel diaphragms 0.010, 0.020, and 0.030 in. thick, respectively.

3.1.2 **The Two-Radii Contour.** – Initial theoretical and experimental studies by Stevens[7] and a more extensive investigation by Cheverton[8] have shown that the volumetric displacement for a given maximum diaphragm stress may be increased if, instead of using the "free-deflection" contour, the diaphragm is forced into a contour plate with the shape shown in cross section in Fig. 8. It is referred to as the two-radii contour because it is specified by the radius of an outer toroidal surface and that of a tangent central spherical surface. The outer constant-radius toroidal surface limits the bending stress at the edge while allowing the bending stress in the remainder of that part of the diaphragm in contact with the toroidal surface to be raised. The maximum stress occurs in the toroidal portion just outside its circle of tangency with the spherical portion. It is believed that, although an optimum contour may exist in which a diaphragm would be equally stressed over its entire area, the two-radii contour and, to a lesser degree, the "free-deflection" contour represent the best practical contours which can be developed and designed without resorting to a very complex analysis and multitudinous machine computations. All pumps described in this report have been designed on the two-radii model.

The following equations permit analysis of the two-radii contour. The notation is given in Fig. 8 and following the equations.

Pump chamber volume from $-Y_0$ to $+Y_0$:

$$V = 4\pi Y_0 R^2 \left[\frac{Z^2}{2} - \frac{Z^3}{4} + \frac{1}{1-Z}\left(\frac{1}{12} - \frac{Z^2}{2} + \frac{2Z^3}{3} - \frac{Z^4}{4}\right)\right] . \tag{6}$$

Radial membrane stress in region A:

$$\sigma_{rm}^{A} = -\frac{EY_0^2}{4R^2Z^2}\left(\frac{x}{R}\right)^2 - \frac{EY_0^2}{R^2(1-Z)^2}\left[\ln Z - Z + \frac{Z^2}{4}\,\frac{1+\nu}{1-\nu} - \frac{Z^3}{6}\,\frac{1+\nu}{1-\nu} + \frac{11-13\nu}{12(1-\nu)}\right] . \tag{7}$$

Radial membrane stress in region B:

$$\sigma_{rm}^{B} = \frac{EY_0^2}{R^2(1-Z)^2}\left[\ln\frac{R}{x} + \frac{4}{3}\left(\frac{x}{R}\right) - \frac{1}{4}\left(\frac{x}{R}\right)^2 + \frac{Z^2}{4}\left(\frac{2}{3}Z - 1\right)\left(\frac{R}{x}\right)^2 + \right.$$

$$\left. + \frac{Z^2}{4}\,\frac{1+\nu}{1-\nu}\left(\frac{2}{3}Z - 1\right) - \frac{11-13\nu}{12(1-\nu)}\right] . \tag{8}$$

---

[7] P. H. Stevens, memorandum to C. B. Graham, "Pulsafeeder Diaphragm Studies," Sept. 24, 1953.

[8] R. D. Cheverton, *Maximum Volume-to-Stress Ratio for a Two-Radii-Contour Diaphragm Pump*, ORNL-2814 (Feb. 1, 1960).

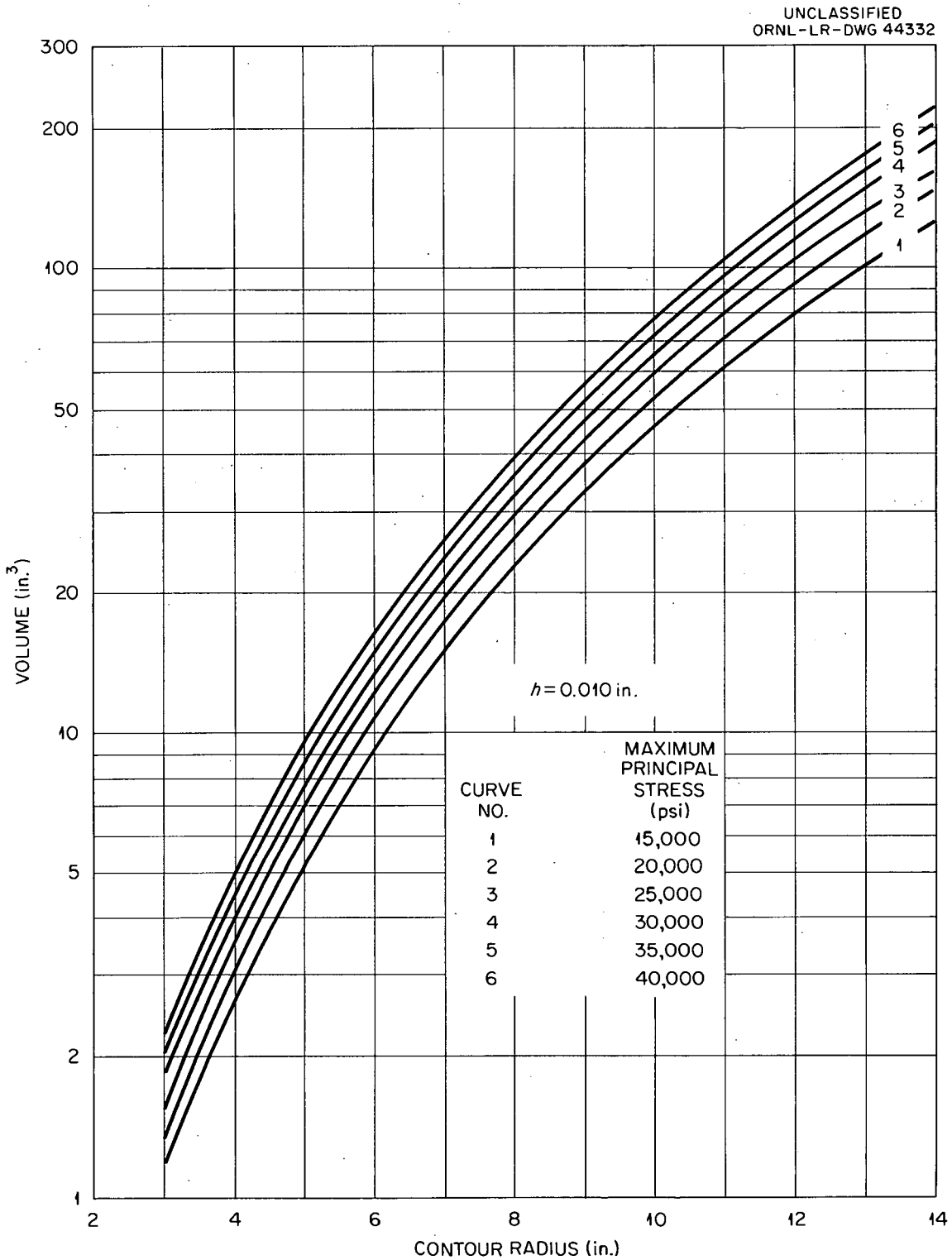

Fig. 5. Maximum Principal Stress in a 0.010-in.-thick Diaphragm in a Free-Deflection Contour.

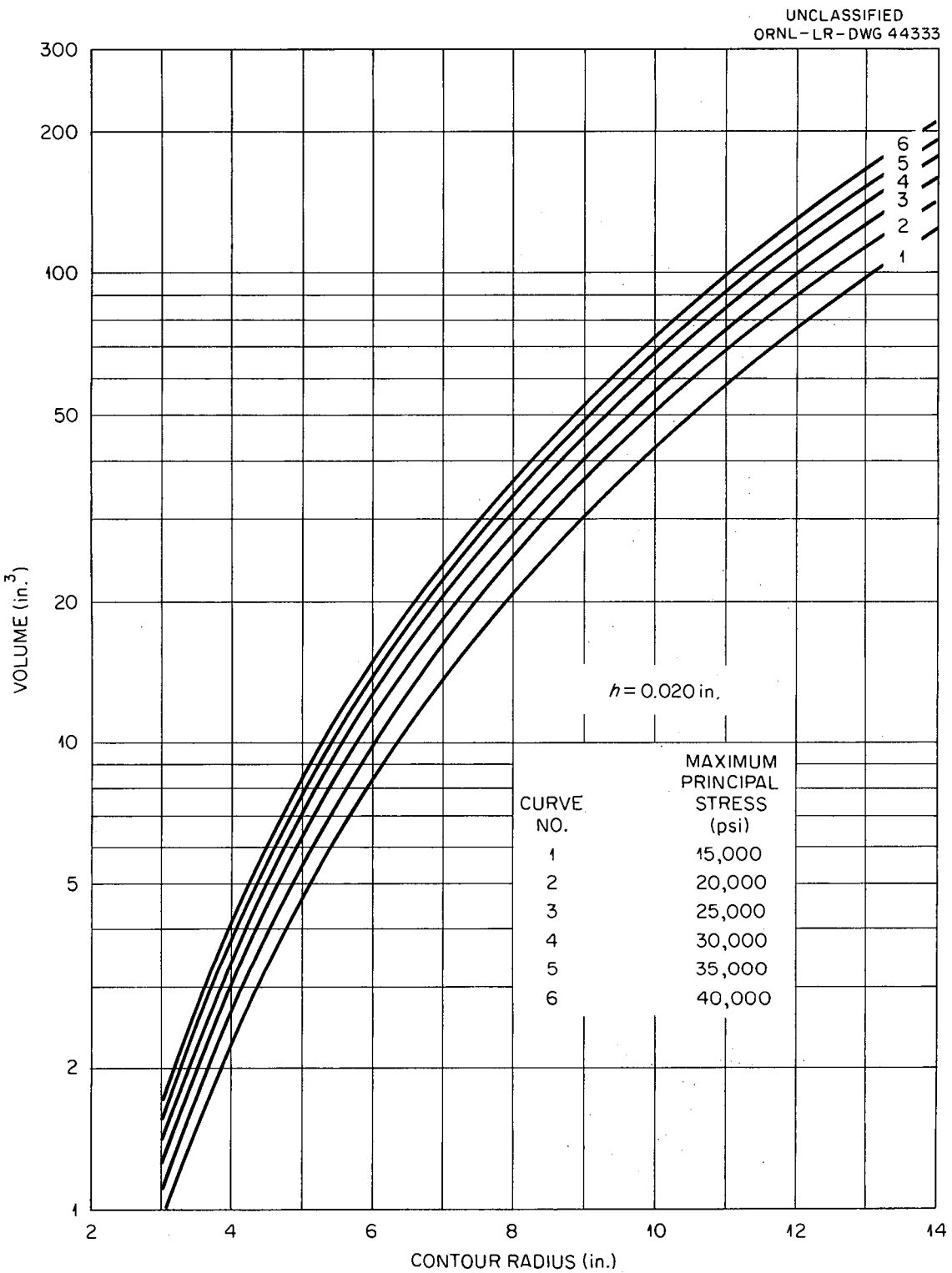

Fig. 6. Maximum Principal Stress in a 0.020-in.-thick Diaphragm in a Free-Deflection Contour.

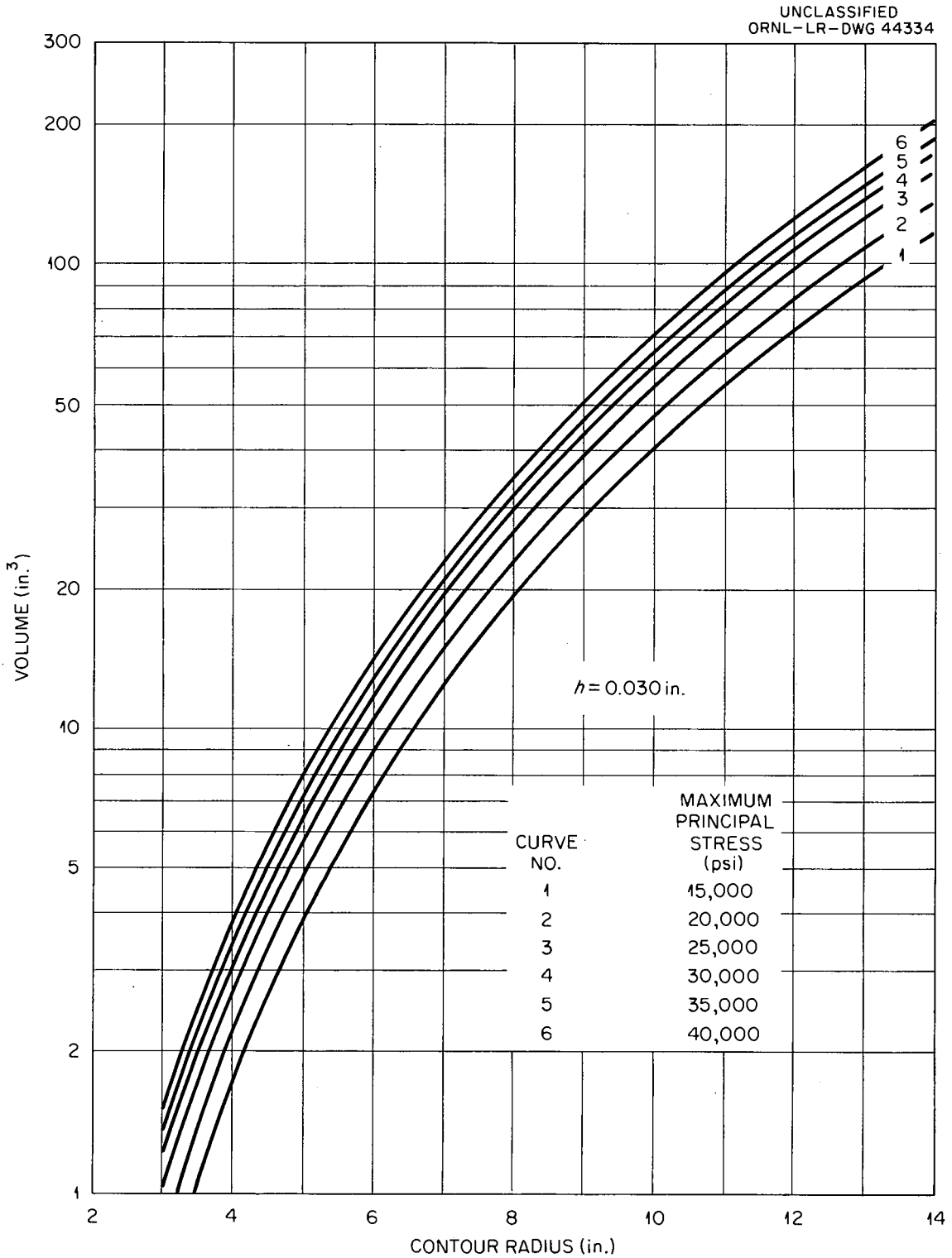

Fig. 7. Maximum Principal Stress in a 0.030-in.-thick Diaphragm in a Free-Deflection Contour.

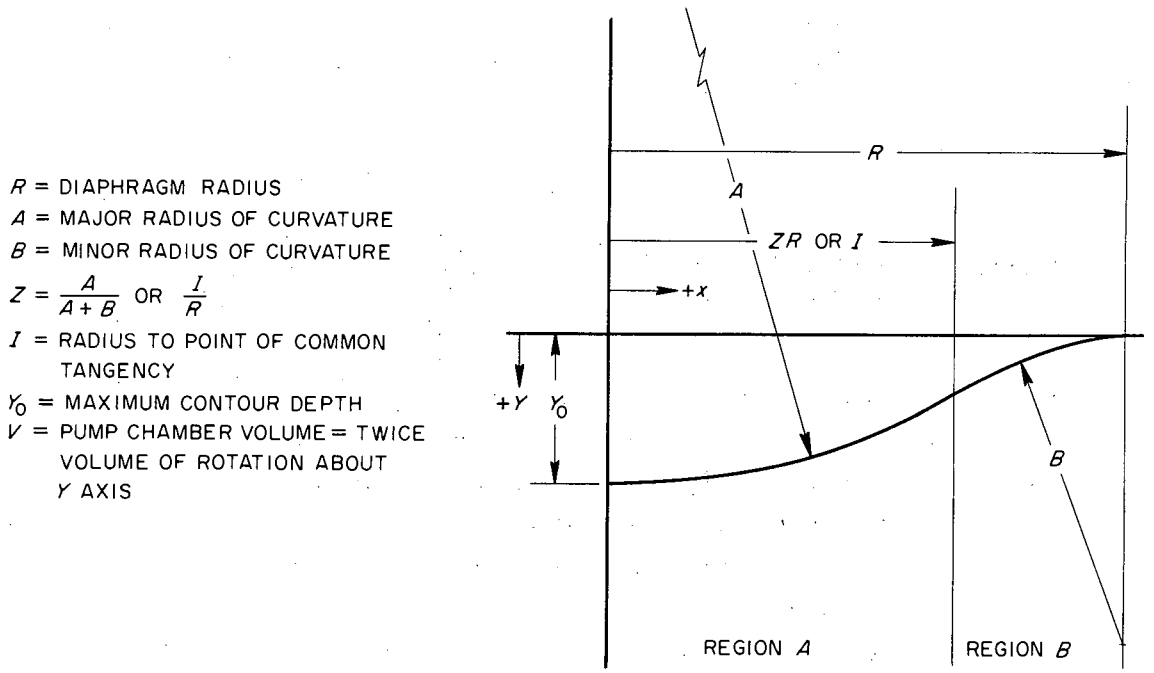

Fig. 8. Description of Two-Radii Contour.

Tangential membrane stress in region A:

$$\sigma_{tm}^{A} = \sigma_{rm}^{A} - \frac{1}{2Z^2}\left(\frac{x}{R}\right)^2 \frac{EY_0^2}{R^2} \quad . \tag{9}$$

Tangential membrane stress in region B:

$$\sigma_{tm}^{B} = \frac{EY_0^2}{R^2(1-Z)^2}\left[\ln\frac{R}{x} + \frac{8}{3}\left(\frac{x}{R}\right) - \frac{3}{4}\left(\frac{x}{R}\right)^2 - \frac{Z^2}{4}\left(\frac{2}{3}Z - 1\right)\left(\frac{R}{x}\right)^2 + \right.$$

$$\left. + \frac{Z^2}{4}\,\frac{1+\nu}{1-\nu}\left(\frac{2}{3}Z - 1\right) - \frac{23 - 25\nu}{12(1-\nu)}\right] \quad . \tag{10}$$

Radial bending stress in region A, σ_{rb}^{A}, equals tangential bending stress in region A, σ_{tb}^{A}:

$$\sigma_{rb}^{A} = \sigma_{tb}^{A} = \frac{EY_0 b}{R^2 Z(1-\nu)} \quad . \tag{11}$$

Radial bending stress in region B:

$$\sigma_{rb}^{B} = \frac{EY_0 b}{R^2(1-Z)(1-\nu^2)}\left[(1+\nu) - \frac{\nu R}{x}\right] \quad . \tag{12}$$

Tangential bending stress in region B:

$$\sigma_{tb}^{B} = \frac{EY_0 b}{R^2(1-Z)(1-\nu^2)}\left[(1+\nu) - \frac{R}{x}\right] . \tag{13}$$

Effective combined stress in fatigue:

$$\sigma_c = \sqrt{\sigma_1^2 + \sigma_2^2 - \sigma_1\sigma_2} . \tag{14}$$

Principal stresses σ_1 and σ_2:

$$\sigma_1 = |\sigma_{rb}| + |\sigma_{rm}| \; ; \qquad \sigma_2 = |\sigma_{tb}| + |\sigma_{tm}| . \tag{15}$$

In the preceding equations, the following nomenclature is used:

Superscript A = region A, the inner, spherical portion of the diaphragm,

Superscript B = region B, the outer, toroidal portion of the diaphragm,

A = radius of inner, spherical portion,

B = cross-sectional radius of toroidal portion,

E = modulus of elasticity,

b = diaphragm thickness,

R = radius of diaphragm (normal to center line),

V = pump chamber volume = twice volume of one contour,

x = distance from center line,

Y_0 = maximum deflection at center line,

$Z = \frac{A}{A+B} = \frac{I}{R}$, where I is distance from center line to circle of tangency between the spherical contour and the toroidal contour,

ν = Poisson's ratio.

In Eq. (14) the Mises-Henly criterion is used for fatigue failure in combined stress, σ_c. Although this expression is for complete reversal of combined stress, whereas the average stress in a diaphragm is displaced above the neutral, it has been selected as a reasonable basis of comparison of contours since it approximates the relation between biaxial stresses and fatigue failure. A more detailed discussion of the correlation of simple reverse-bending endurance stress with combined stress plus a displaced average stress is given by Cheverton[8] and by texts on the subject. In general, they are proportional to each other. The allowable stress is chosen on the basis of experience, taking into account the endurance limit of the material in its intended environment, the desired operating life, and such expected deviations from ideal conditions as irregularities in the dynamic behavior of the diaphragm and the presence of solid particles in the process fluid.

It is found that the optimum value of Z, and therefore the optimum ratio of A to B, is a function of b/Y_0. The fact that the ratio of A to B is a dependent variable considerably simplifies the design of a two-radii contour and made possible the parameter studies of Figs. 9–20.

In Fig. 9 the dimensionless volume-stress ratio $VEY_0/2R^4\sigma_c$ is plotted vs Z. Figure 10 is a plot of the ratio h/Y_0 vs the dimensionless ratio V/R^3 for various maximum combined stress levels. These plots were obtained as follows.

The volume swept by the diaphragm from $-Y_0$ to $+Y_0$ is

$$V = 4\pi Y_0 R^2 \left[\frac{Z^2}{2} - \frac{Z^3}{4} + \frac{1}{1-Z}\left(\frac{1}{12} - \frac{Z^2}{2} + \frac{2Z^3}{3} - \frac{Z^4}{4}\right)\right] . \tag{6}$$

With the definition

$$f(Z) = \frac{Z^2}{2} - \frac{Z^3}{4} + \frac{1}{1-Z}\left(\frac{1}{12} - \frac{Z^2}{2} + \frac{2Z^3}{3} - \frac{Z^4}{4}\right) , \tag{16}$$

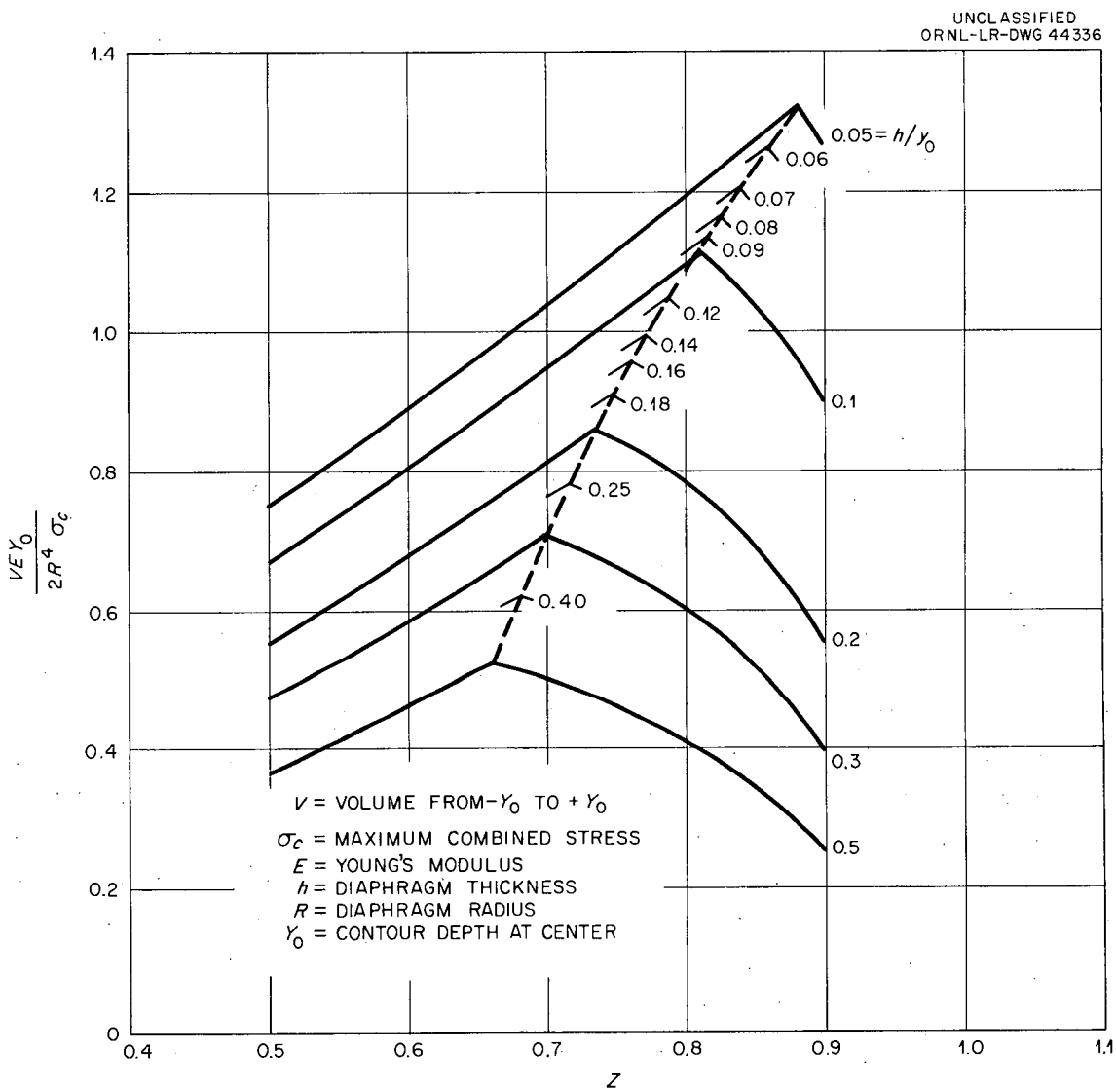

Fig. 9. Volume-Stress Ratio vs Z for Various Values of h/Y_0.

Eq. (6) gives

$$Y_0 = \frac{V}{4\pi R^2 f(Z)} \quad . \tag{17}$$

For given values of h/Y_0 and Z, the value of the dimensionless ratio

$$\frac{VEY_0}{2R^4 \sigma_c} = C_1 \tag{18}$$

can be taken from Fig. 9. In terms of this ratio,

$$V = \frac{2C_1 \sigma_c R^4}{EY_0} \quad . \tag{19}$$

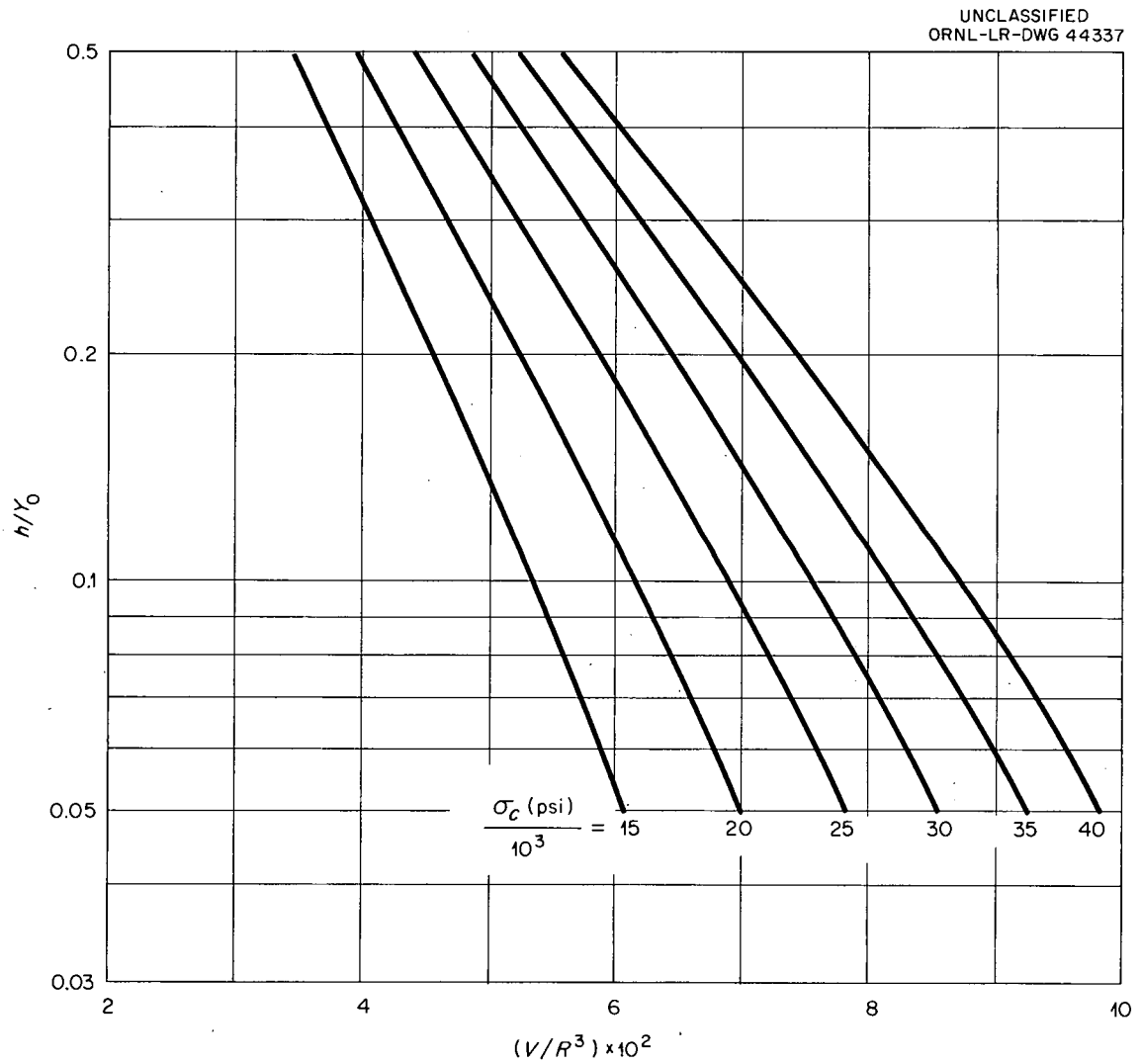

Fig. 10. Plot of h/Y_0 vs V/R^3.

Upon eliminating Y_0 from Eqs. (17) and (19) and reducing,

$$V = R^3 \sqrt{\frac{8C_1 \pi \sigma_c f(Z)}{E}} \quad .$$

Values of the dimensionless ratio

$$\frac{V}{R^3} = \sqrt{\frac{8C_1 \pi \sigma_c f(Z)}{E}}$$

are given in Table 1 and are plotted in Fig. 10. These plots may be interpolated to obtain values corresponding to specific diaphragm thicknesses, b/Y_0, other than those presented in Figs. 11–20.

Figures 11–20 are plots of the swept volume as a function of diaphragm radius for various values of b/Y_0, Z, and combined stress, σ_c. The diaphragm thickness b may be read directly by means of the superposed dashed lines. From these values, the contour depth Y_0 is readily obtainable, since

$$Y_0 = \frac{b}{b/Y_0} \quad .$$

The contour radii can be obtained by means of the relations

$$A = \frac{Z(Y_0^2 + R^2)}{2Y_0} \quad , \qquad B = \frac{A}{Z} - A \quad .$$

The HRT feed and purge pumps are two examples of pumps which have been put into service. The contours were adapted from Lapp Pulsafeeder pumps and modified to reduce the stress level. The description of the contours and the calculated stresses with type 347 stainless steel diaphragms are given in Table 2.

Table 1. Volumetric Displacement of Two-Radii-Contour Pumps

$\frac{b}{Y_0}$	Z^a	$C_1{}^{a,b}$	$f(Z)^c$	V/R^3 for the Indicated Maximum Combined Stress Levels (psi)					
				15,000	20,000	25,000	30,000	35,000	40,000
				$\times 10^{-2}$	$\times 10^{-2}$	$\times 10^{-2}$	$\times 10^{-2}$	$\times 10^{-2}$	$\times 10^{-2}$
0.05	0.880	1.320	0.2195	6.03	6.98	7.80	8.55	9.23	9.85
0.10	0.810	1.110	0.2040	5.35	6.17	6.90	7.54	8.16	8.70
0.20	0.735	0.860	0.1895	4.54	5.24	5.85	6.41	6.92	7.40
0.30	0.700	0.710	0.1823	4.04	4.65	5.22	5.71	6.17	6.60
0.50	0.660	0.525	0.1753	3.41	3.93	4.30	4.86	5.20	5.55

[a]Values taken from Fig. 9.
[b]Defined in Eq. (18).
[c]Defined in Eq. (16).

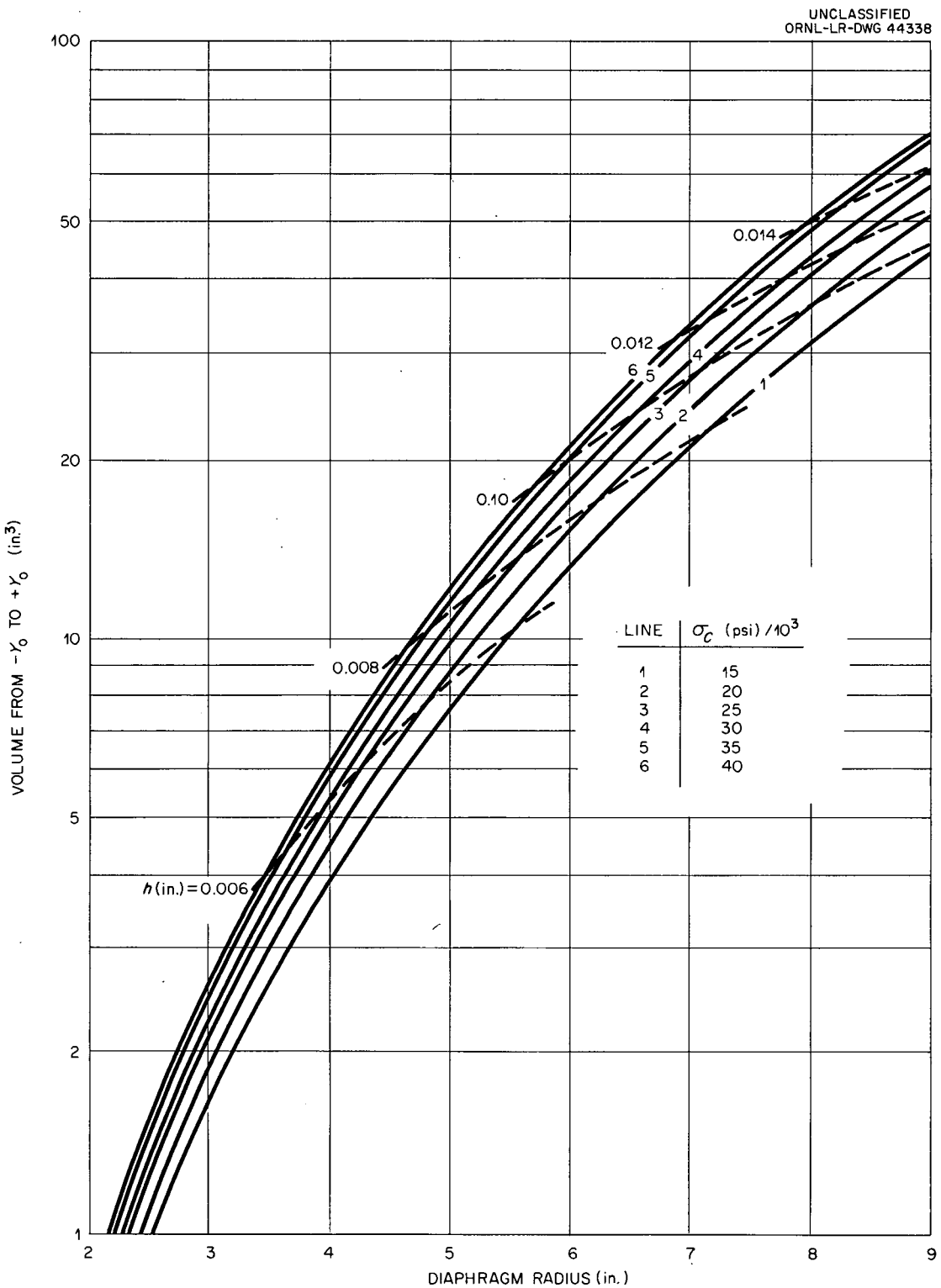

Fig. 11. Volumetric Displacement vs Diaphragm Radius for Two-Radii Contour with $h/Y_0 = 0.05$ and $Z = 0.88$.

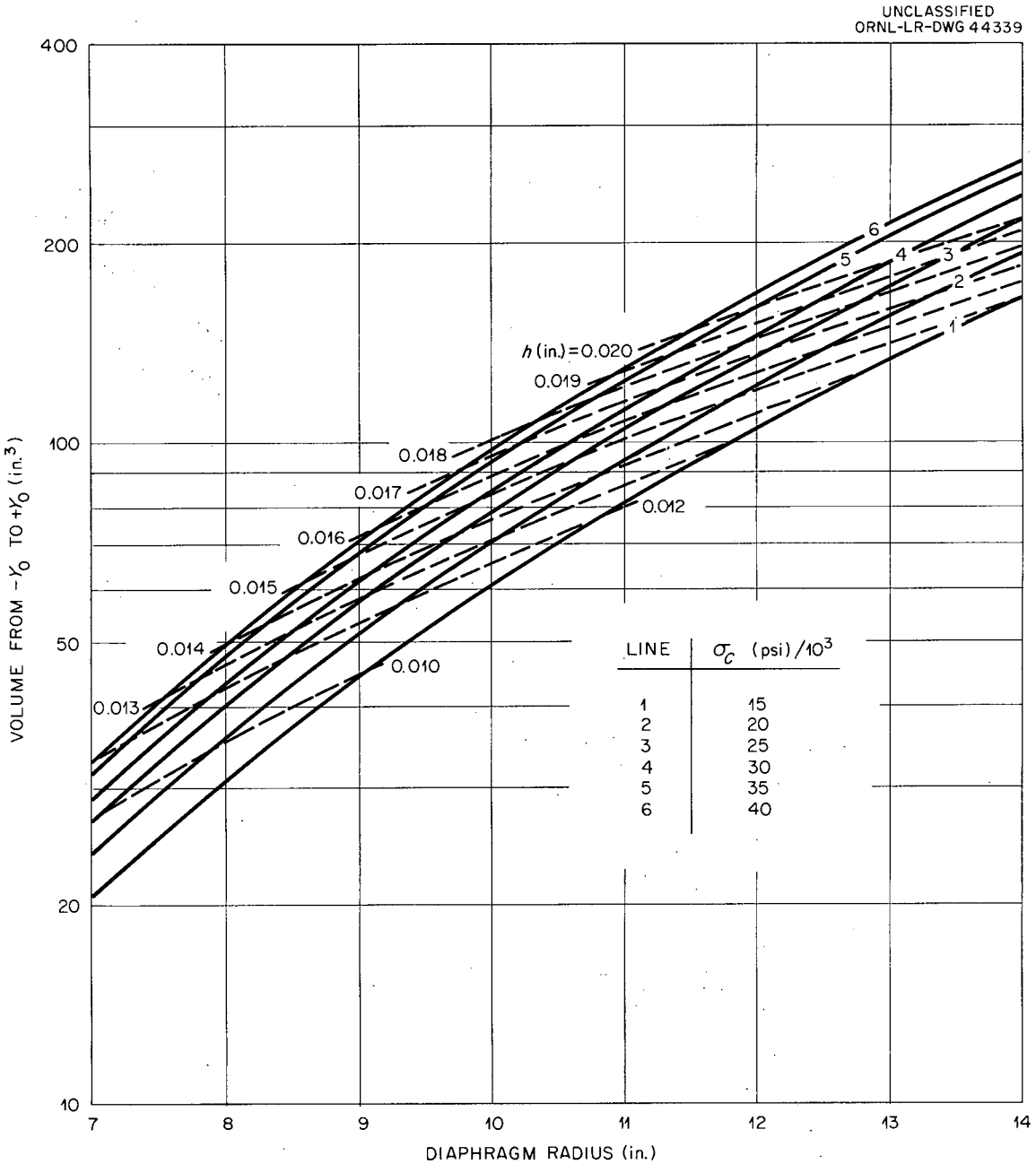

Fig. 12. Volumetric Displacement vs Diaphragm Radius for Two-Radii Contour with $h/Y_0 = 0.05$ and $Z = 0.88$ (Continuation of Fig. 11).

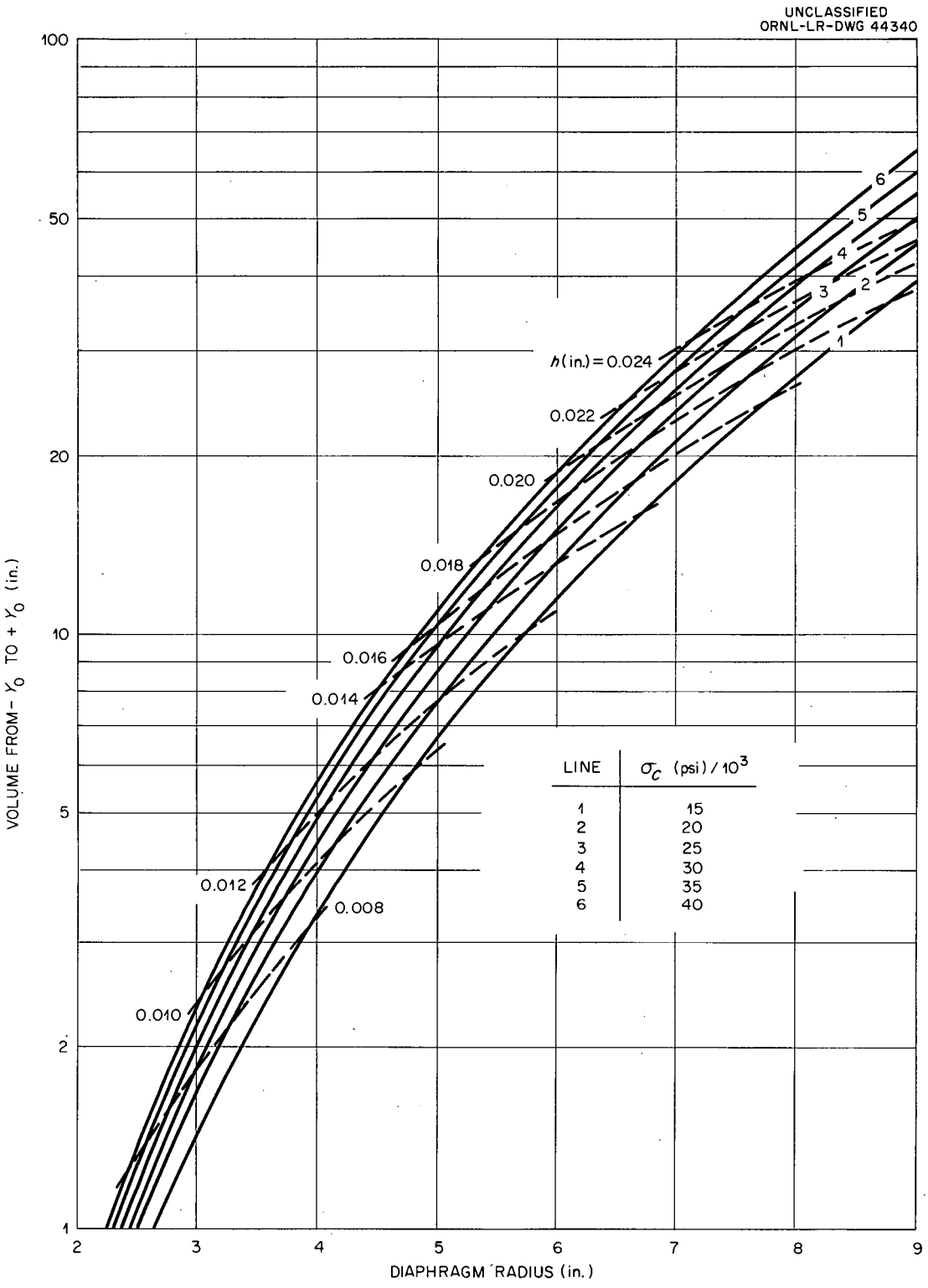

Fig. 13. Volumetric Displacement vs Diaphragm Radius for Two-Radii Contour with $h/Y_0 = 0.10$ and $Z = 0.81$.

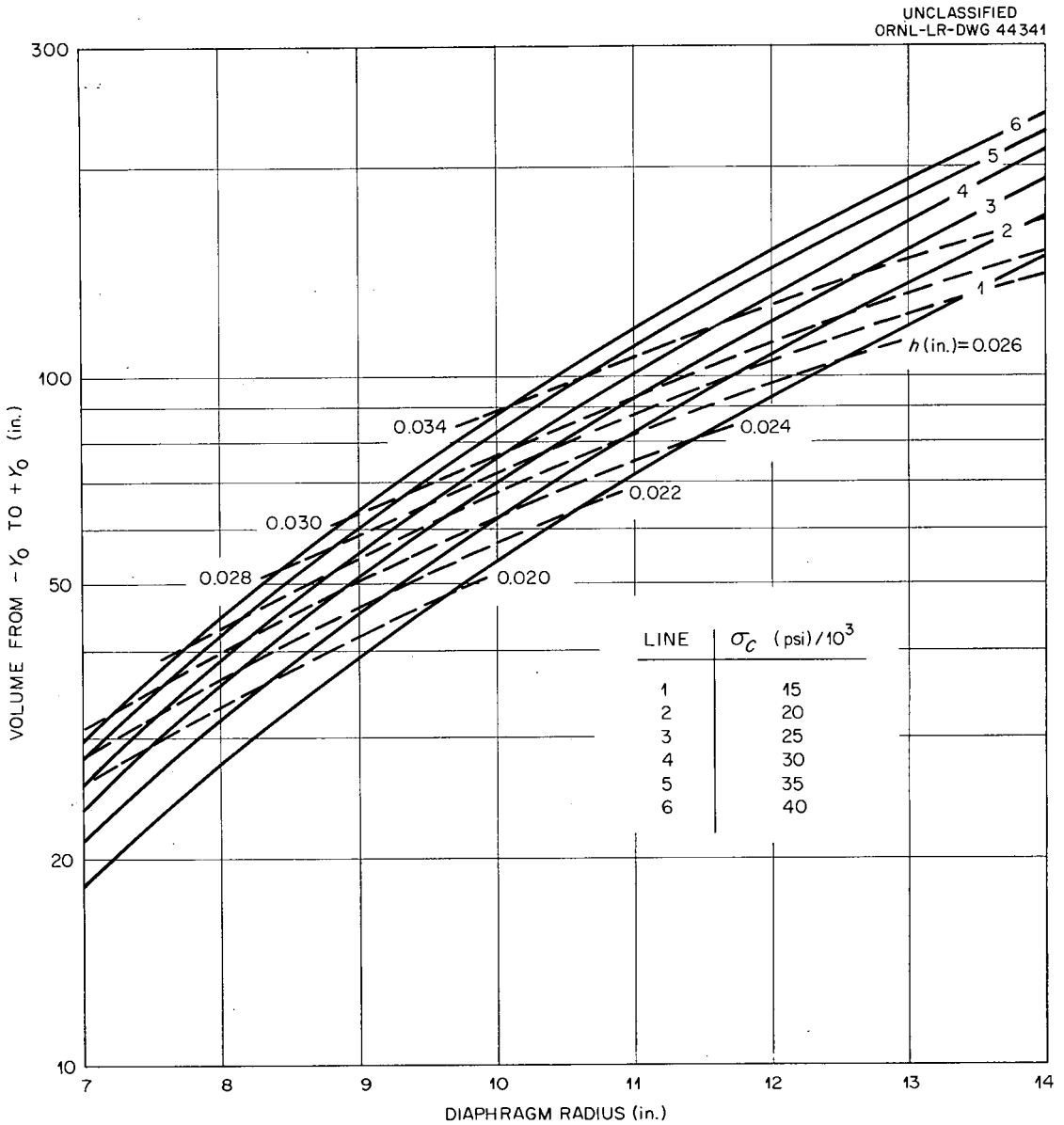

Fig. 14. Volumetric Displacement vs Diaphragm Radius for Two-Radii Contour with $h/Y_0 = 0.10$ and $Z = 0.81$ (Continuation of Fig. 13).

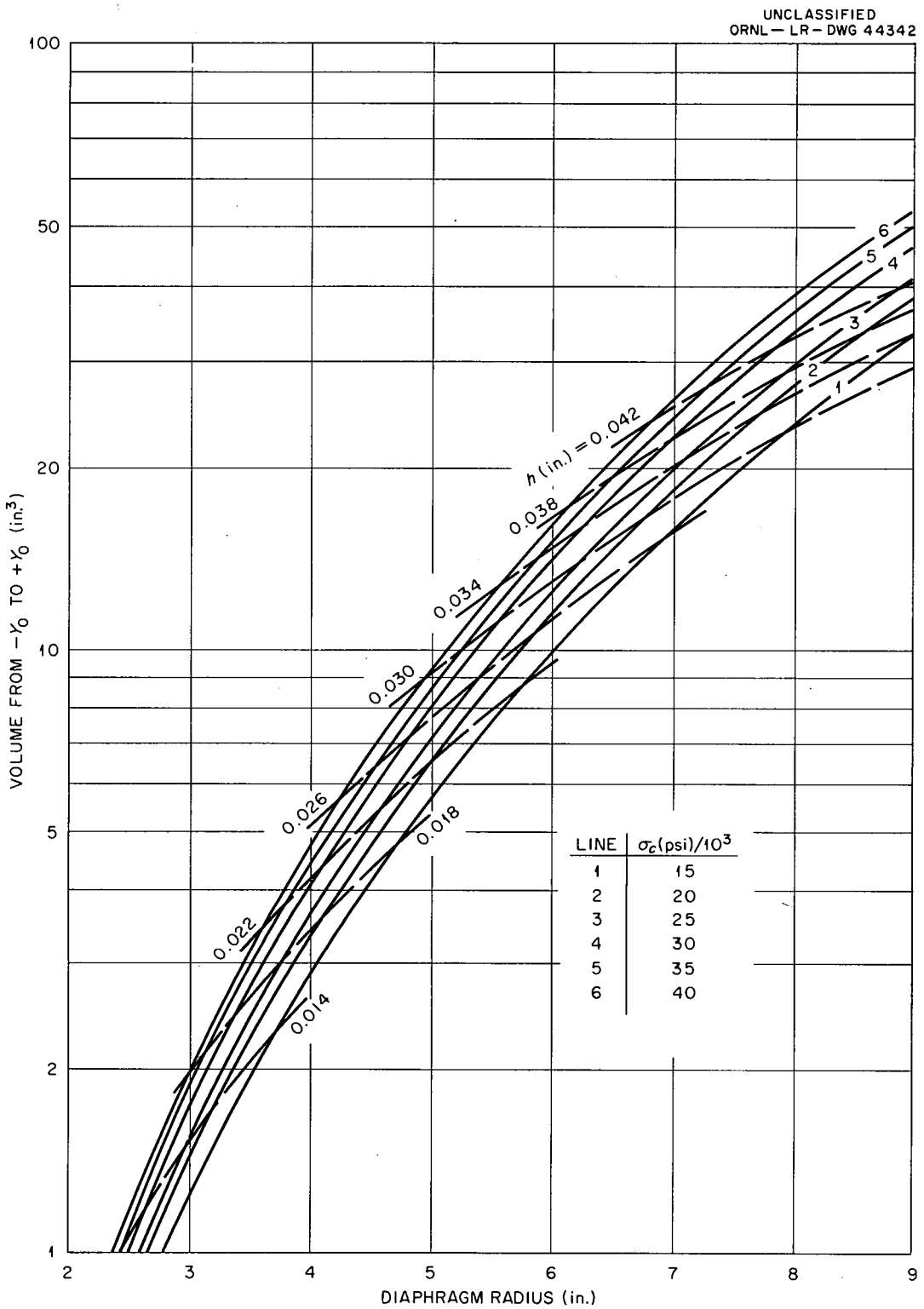

Fig. 15. Volumetric Displacement vs Diaphragm Radius for Two-Radii Contour with $h/Y_0 = 0.20$ and $Z = 0.735$.

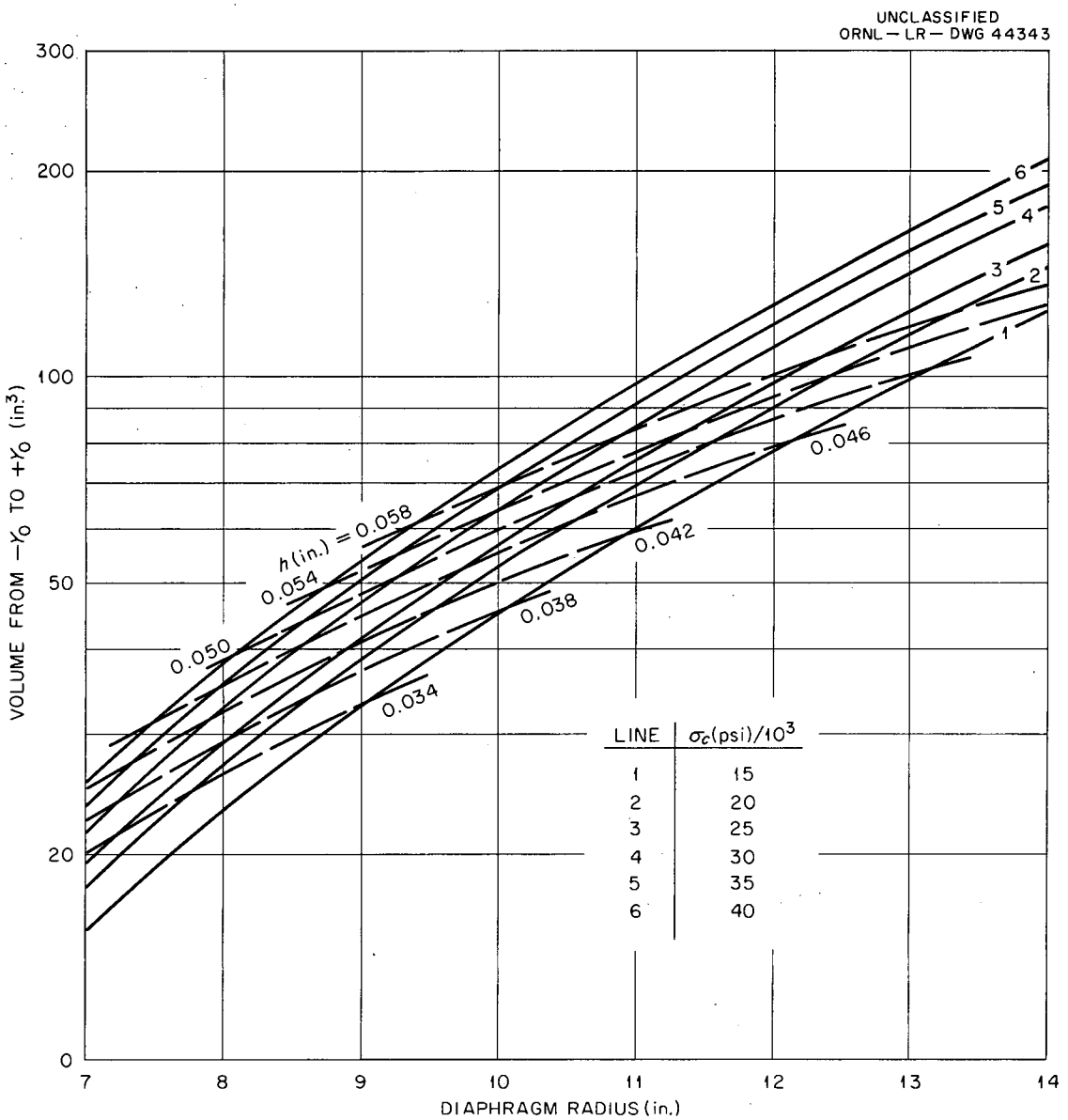

Fig. 16. Volumetric Displacement vs Diaphragm Radius for Two-Radii Contour with $b/Y_0 = 0.20$ and $Z = 0.735$ (Continuation of Fig. 15).

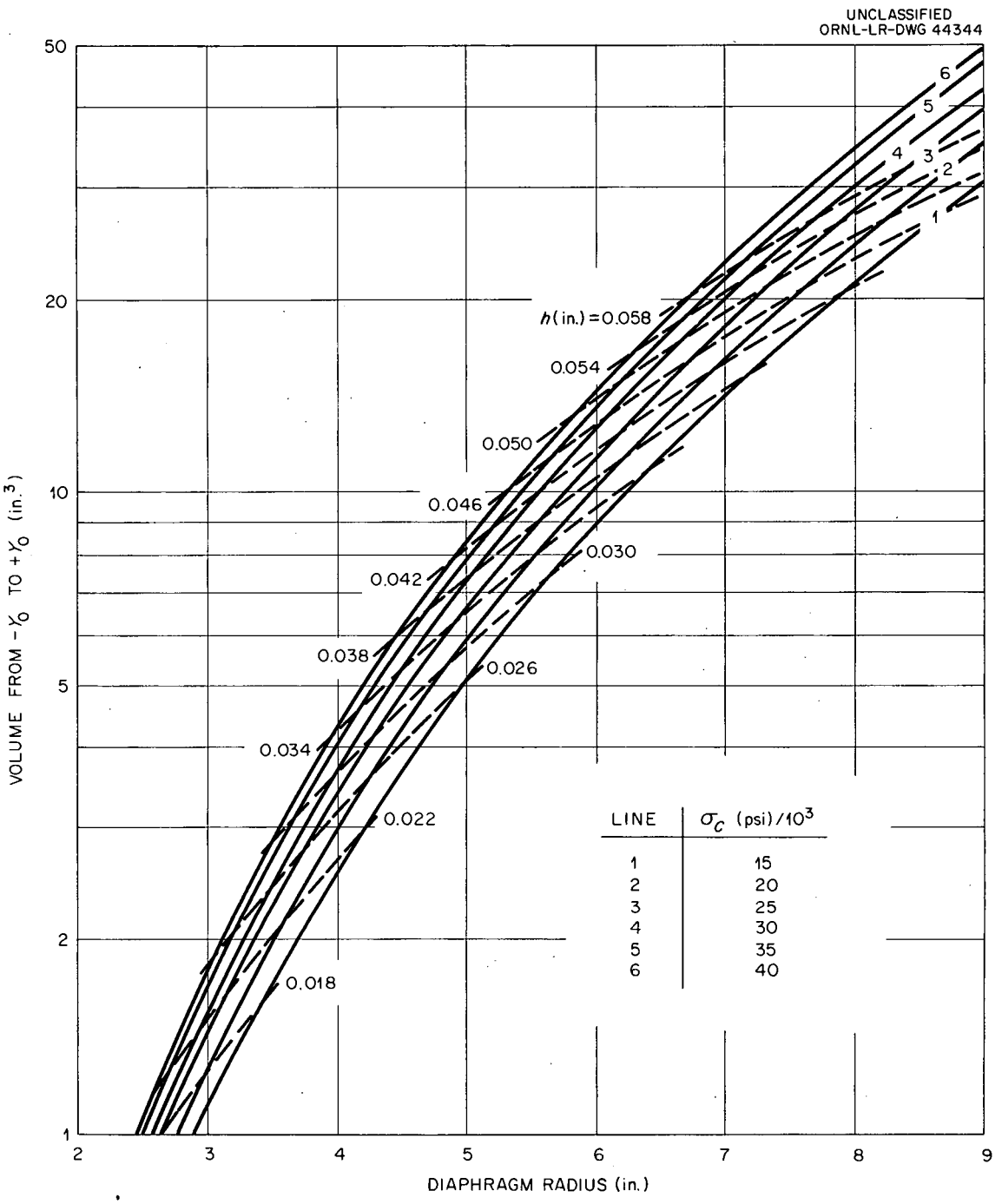

Fig. 17. Volumetric Displacement vs Diaphragm Radius for Two-Radii Contour with $h/Y_0 = 0.30$ and $Z = 0.700$.

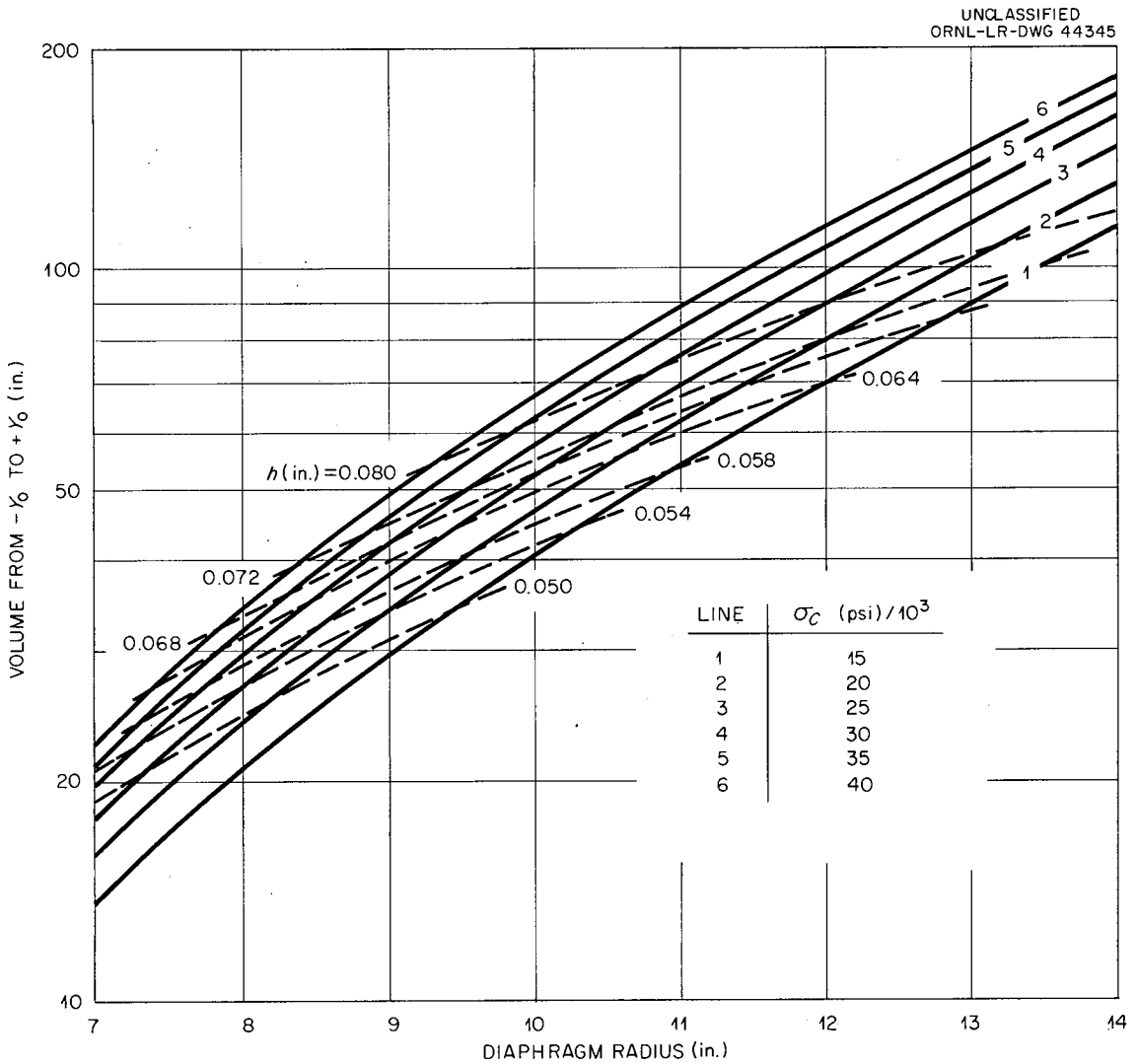

Fig. 18. Volumetric Displacement vs Diaphragm Radius for Two-Radii Contour with h/Y_0 = 0.30 and Z = 0.700 (Continuation of Fig. 17).

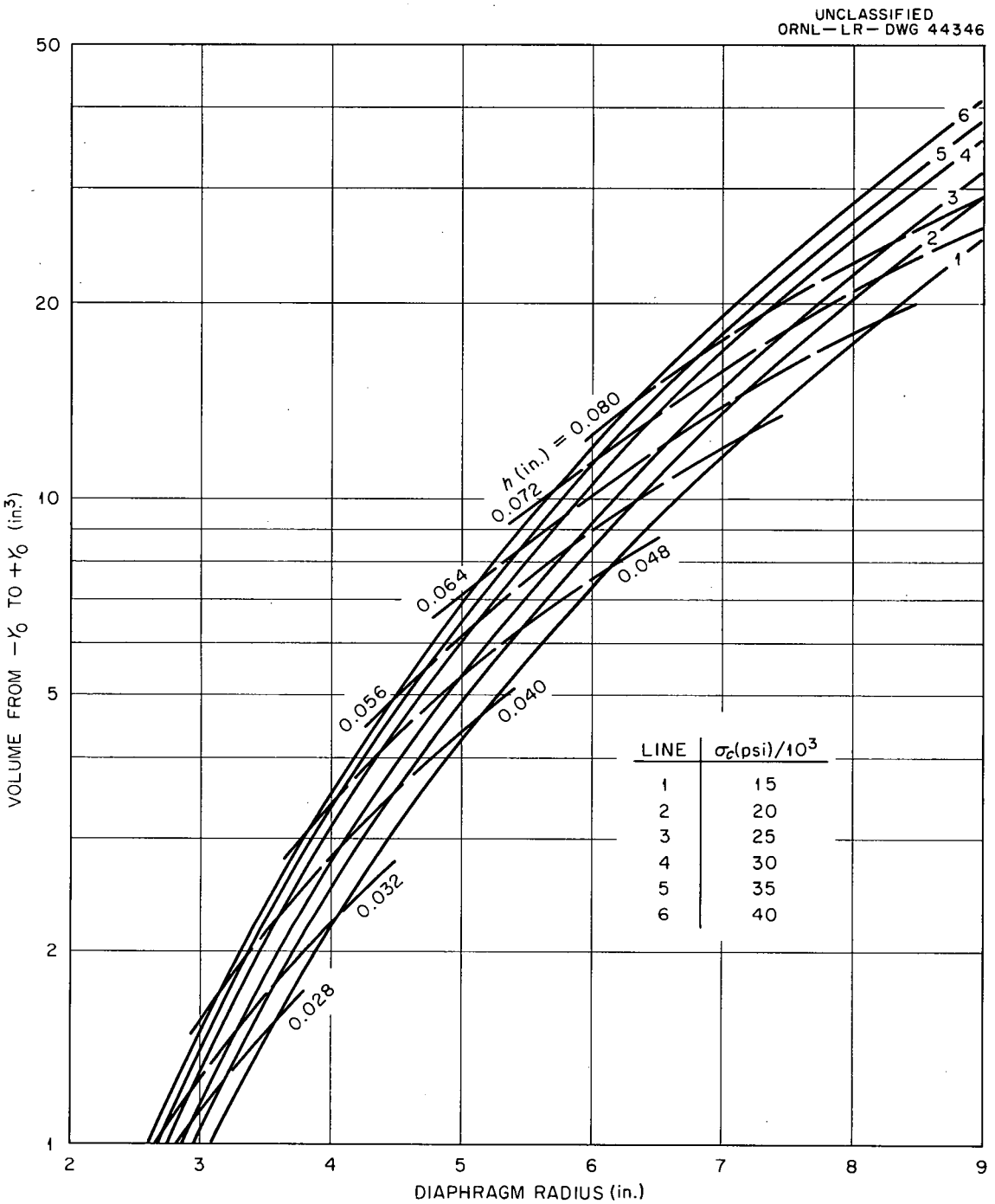

Fig. 19. Volumetric Displacement vs Diaphragm Radius for Two-Radii Contour with $h/Y_0 = 0.50$ and $Z = 0.66$.

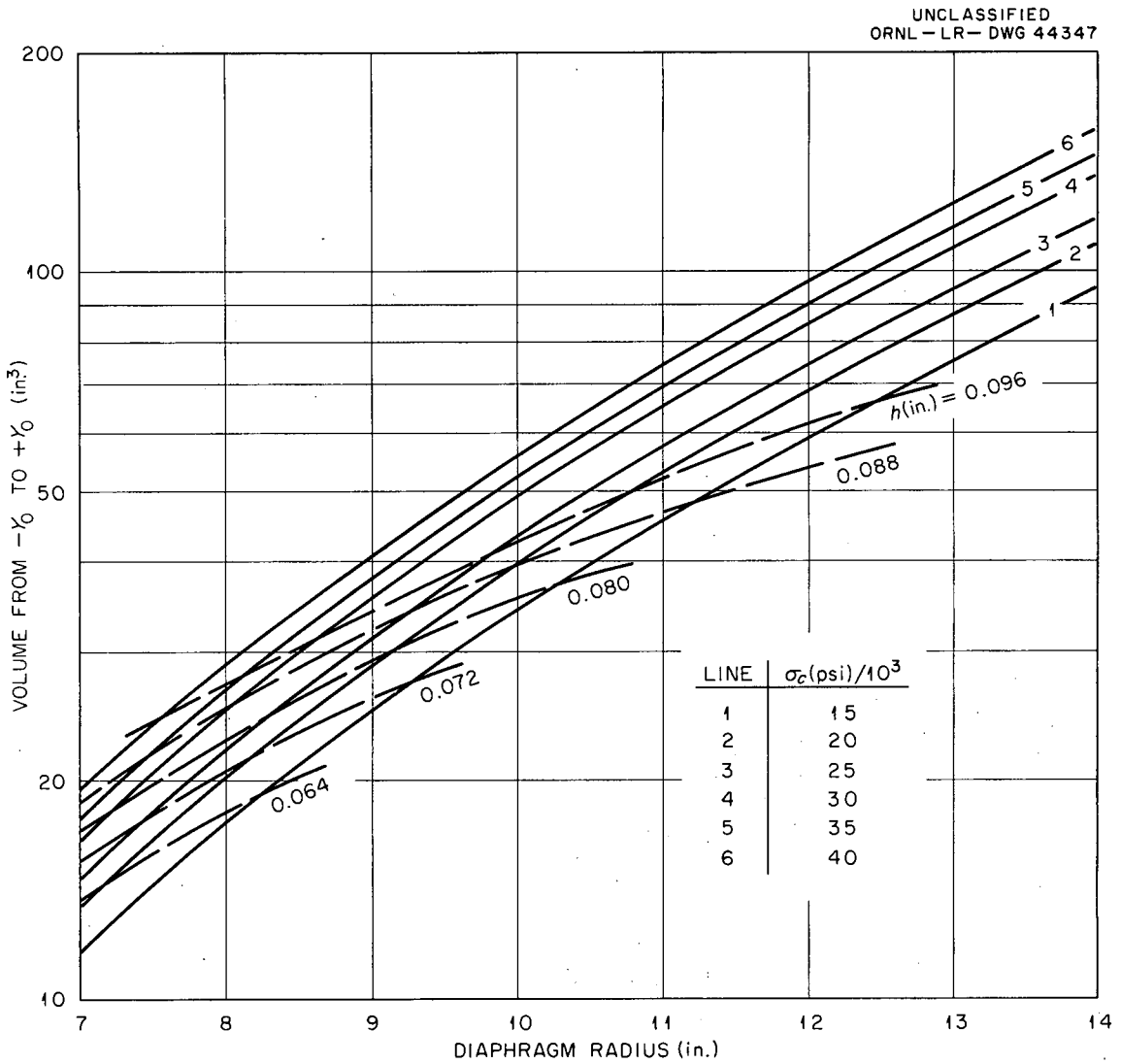

Fig. 20. Volumetric Displacement vs Diaphragm Radius for Two-Radii Contour with $h/Y_0 = 0.50$ and $Z = 0.66$ (Continuation of Fig. 19).

Table 2. Characteristics of HRT Diaphragm Pumps

Dimension or Stress	Feed Pump*	Purge Pump**
R, in.	5.375	2.750
A, in.	112.5	~43
B, in.	32.0	~18
h, in.	0.031	0.019
Y_0, in.	0.100	0.0672
σ_{rm} max, psi	9,833 at $x/R = 0.1$	17,227 at $x/R = 0.1$
σ_{rb} max, psi	14,943 at $x/R = 1$	18,230 at $x/R = 1$
σ_1 max, psi	21,054 at $x/R = 0.8$	28,944 at $x/R = 0.7$

*Exact two-radii contour.

**Approximate two-radii contour.

3.1.3 **Factors Affecting the Dynamic Behavior of Diaphragms.** – In order that the stresses in the diaphragm not exceed the theoretical level for full deflection into the contour, it is necessary that the diaphragm travel smoothly and uniformly from contour to contour. Continuous physical measurement[9] of the motion of diaphragms in an HRT pump head operating at rated conditions revealed two types of irregularities occurring during each stroke and contributing flexures and stresses well above what would be expected. The first irregularity was a fluttering motion evident in three diaphragm follower traces (lower right, Fig. 21) in which the diaphragm, rather than proceeding smoothly across the cavity, was moving forward, backward, and forward again many times in the course of one stroke. These flutters occurred at the same time as pressure variations, indicative of hammer or standing waves, evident in the pressure-time trace taken on the Scott and Williams P9 hydraulic drive system (see Sec 7.1). Substitution of a reciprocating drive appreciably reduced the flutter in the pressure and diaphragm traces (Fig. 22), and as discussed in Sec 7.1, modifications[10] to the slide valve of the Scott and Williams unit accomplished the same result.

The second irregularity was the nonuniform progression of the diaphragm (Figs. 21 and 22 and in more detail in ref 9) from the driving contour plate to the pumping contour plate, forming a belly and short reverse bend which moved downward as the diaphragm progressed to the right. This reverse bend appeared to reach its point of shortest radius, thereby creating the highest bending stress, in the area where the majority of the diaphragm failures have occurred. So that

[9]R. Blumberg, C. Gabbard, and E. C. Hise, *Diaphragm Feed Pump Development Program Progress Report*, ORNL CF-56-10-114 (Oct. 29, 1956).

[10]H. R. Payne, *Modification of Oil Control Valve in Scott and Williams P9 Pulsator Drive*, ORNL CF-58-1-65 (Jan. 14, 1958).

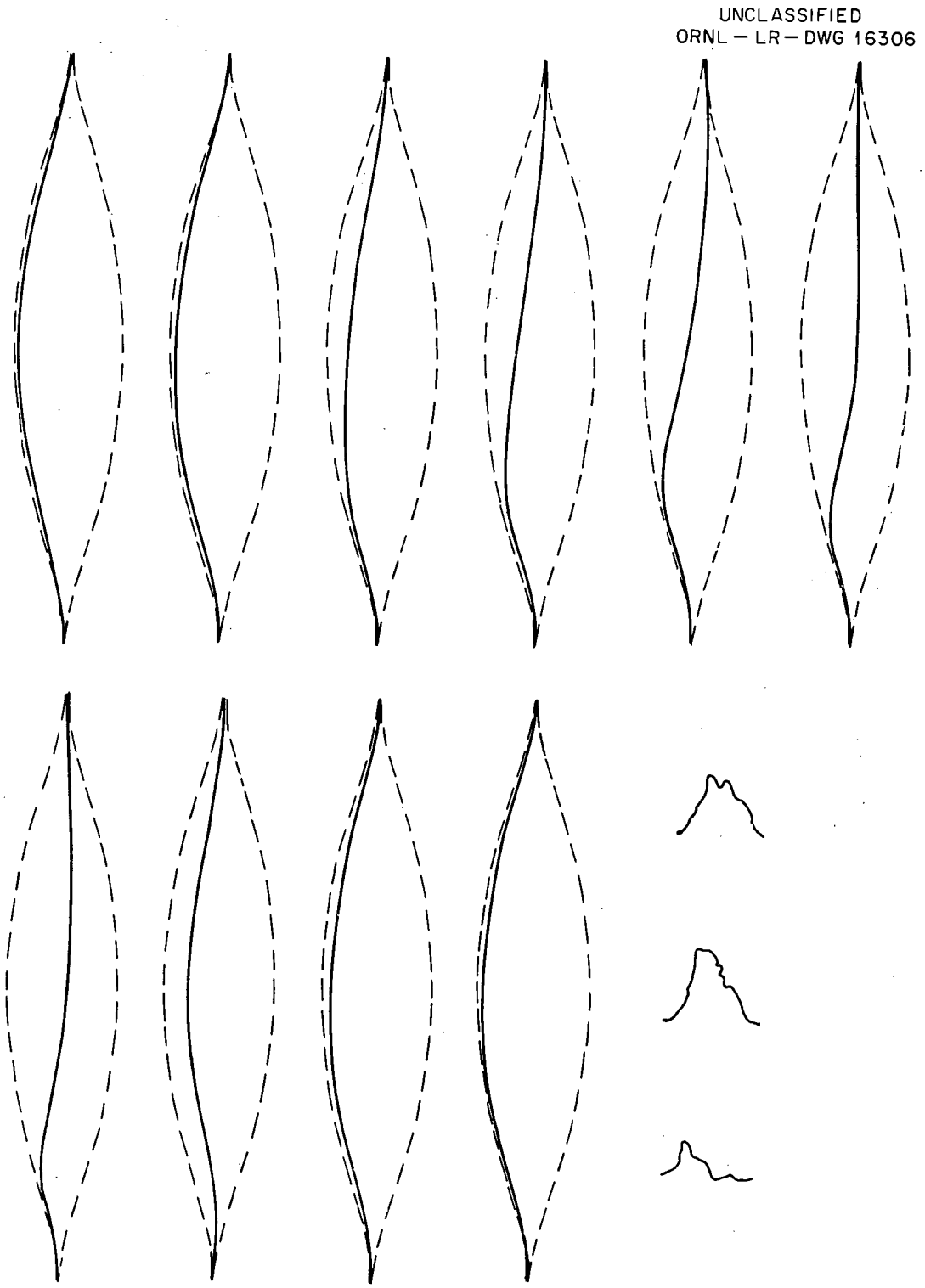

Fig. 21. Diaphragm Motion Through One Cycle for a 0.019-in.-thick Diaphragm of Annealed Type 347 Stainless Steel. Discharge pressure, 2000 psi; stroke volume, 3 in.^{3}; speed, 78 strokes/min; Scott and Williams drive.

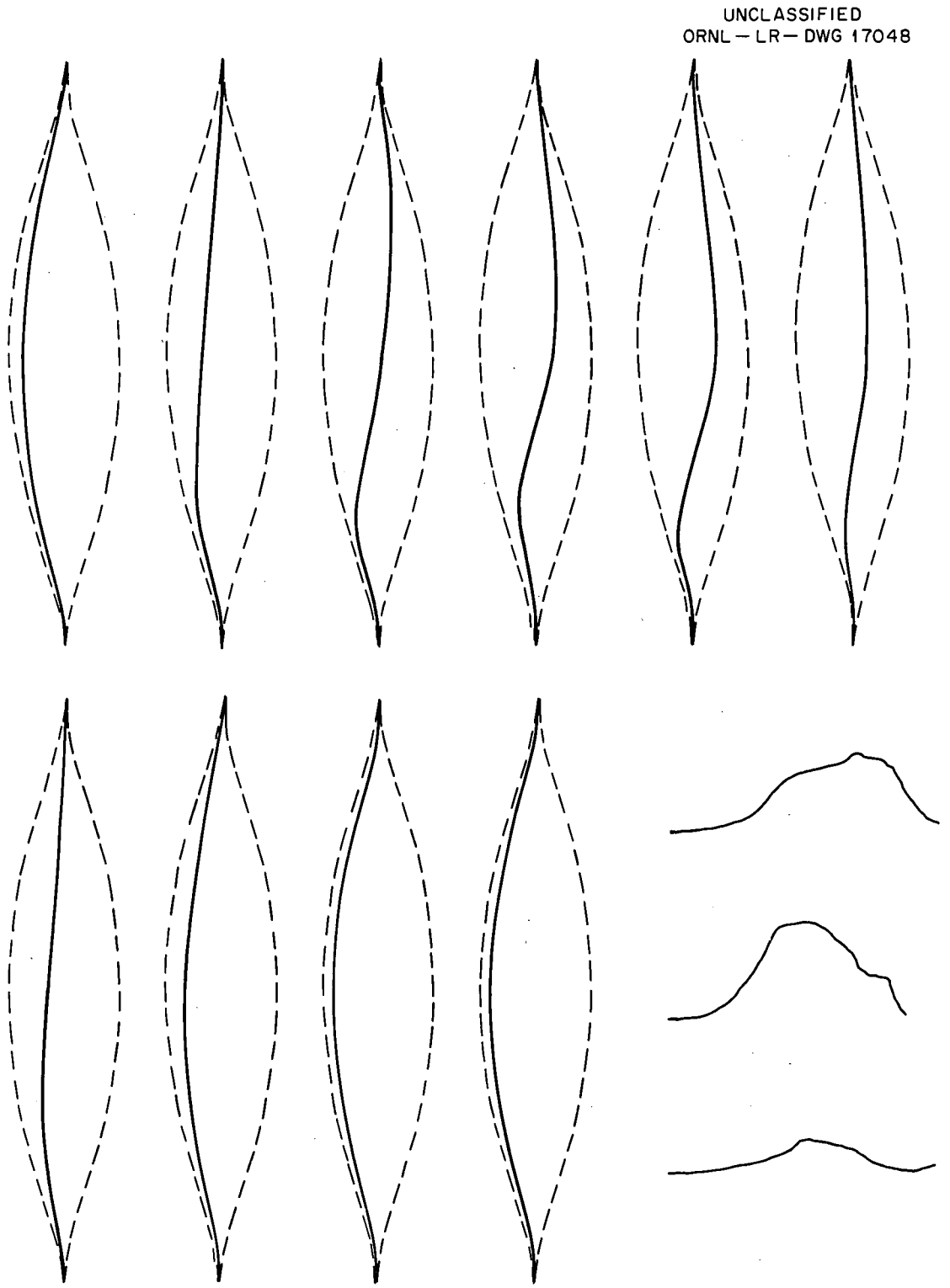

Fig. 22. Diaphragm Motion Through One Cycle for a 0.019-in.-thick Diaphragm of Annealed Type 347 Stainless Steel. Discharge pressure, 2000 psi; stroke volume, 2.3 in.^{3}; speed, 56 strokes/min; reciprocating drive.

the HRT head would be as simple and rugged as possible and at the same time permit no possibility of gas entrapment in the head, the drive-line entrance and the discharge-line exit had been placed at the top of the pump cavity. This apparently created sufficient hydraulic unbalance to cause the unsymmetrical displacement of the 0.019-in.-thick diaphragm. Since it was not desirable to alter the head design, a 0.031-in.-thick diaphragm was installed to reduce the effect of the hydraulic unbalance. Figure 23 demonstrates the action of the stiffer diaphragm. Calculations indicate that the theoretical stress in the 0.031-in.-thick diaphragm is about 5000 psi higher than in the one 0.019 in. thick. The actual stress in the unsymmetrically deformed 0.019-in. diaphragm cannot be readily measured or calculated. The fact that the average life of the 0.031-in. diaphragm is greater than that of the 0.019-in. diaphragm (Table 4) is presumed to be largely due to a lower actual stress in the thicker diaphragm.

Recent experimental head designs (Fig. 24) at ORNL and most commercial head designs attempt to introduce the liquid to the pump cavity in a symmetrical fashion so as not to require any rigidity from the diaphragm. The following general guides can be expected to lead to good hydraulic design:

1. The drive unit should create no standing waves or water hammer.
2. The entry of the drive, suction, and discharge lines to the pump chamber should be diffused so as not to impinge upon the diaphragm.
3. The passages communicating through the contour should be arranged with regard to the fact that two-thirds of the volumetric displacement occurs in the band from $R/3$ to $2R/3$.

3.1.4 **Diaphragm Materials.** – The diaphragm metal is selected principally on the basis of its endurance limit in the intended environment of application. Spring steels, stainless steels, and phosphor bronze have been used successfully by manufacturers for various applications, and other materials such as titanium merit further investigation. Type 347 stainless steel was chosen for the diaphragm material for the feed and purge pumps in the HRT.

In order to compare the endurance limit of annealed type 347 stainless steel with other possible diaphragm materials in the uranyl sulfate fuel solution, a research contract was undertaken by Ohio State University.[11] Standard sheet specimens were operated in reverse bending in air, distilled water, and fuel solution. A summary of the results is shown in Table 3. The preliminary tests run in air agreed well with values found in the literature, establishing the validity of the tests. Although work hardening improved the endurance limit of austenitic stainless steels in air and distilled water, it decreased the endurance limit in the fuel solution. Some of the hardenable stainless steel alloys, for example, AM-350 SBT, were superior to type 347 in air and water and showed some improvement in fuel. Titanium had a very high endurance limit in all three environments; however, it is known to be unusually notch sensitive. A series of tests,[11] not shown in the table, made to determine the effects of scratches on type 347 specimens indicated no notch sensitivity, although experience has shown that most failures

[11] F. H. Beck, *Fatigue and Corrosion Fatigue of Stainless Steel by Uranyl Sulfate*, Engineering Experiment Station, Ohio State University (May 14, 1958).

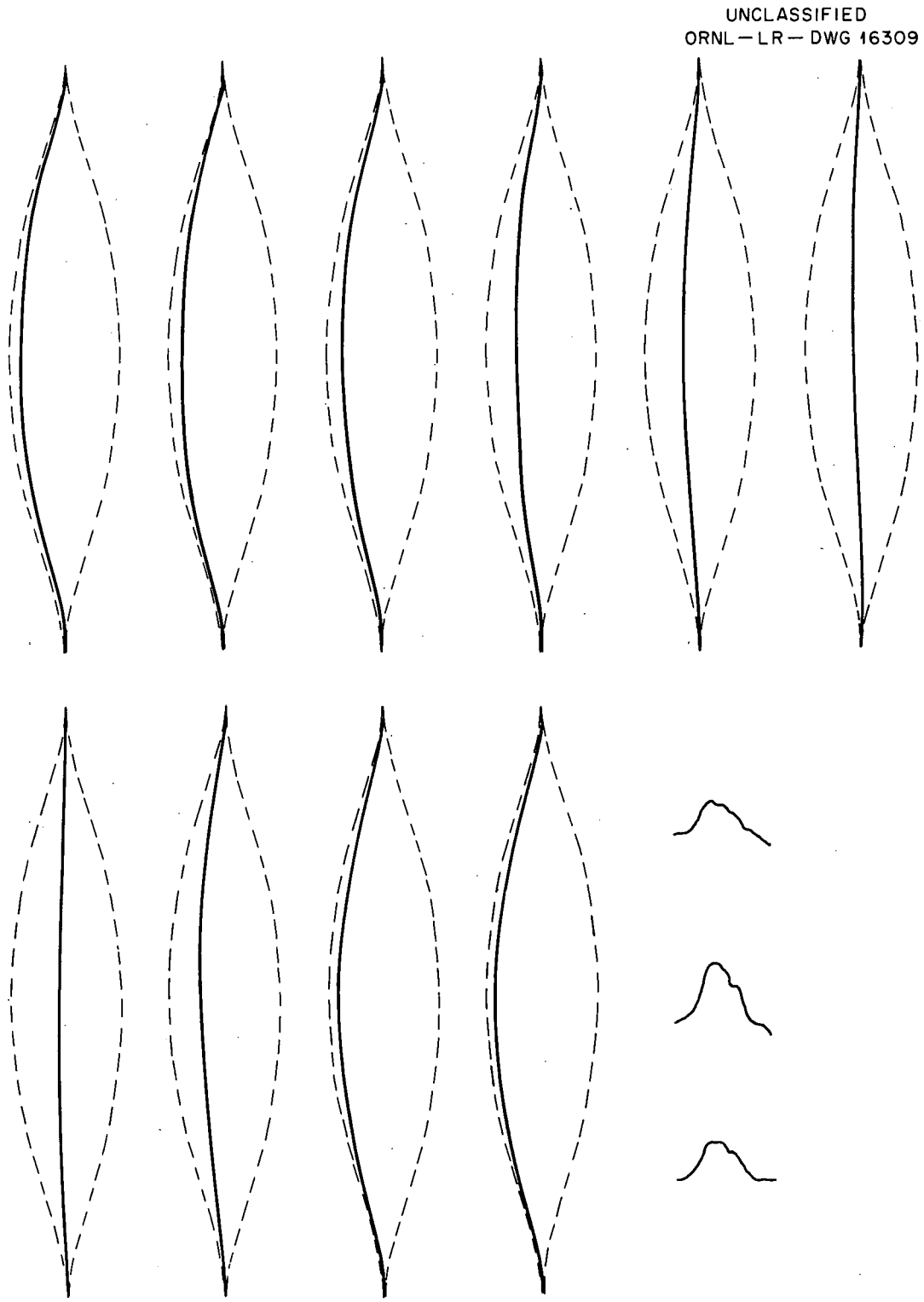

Fig. 23. Diaphragm Motion Through One Cycle for a 0.031-in.-thick Diaphragm of Annealed Type 347 Stainless Steel. Discharge pressure, 2000 psi; stroke volume, 2.4 in.^{3}; speed, 78 strokes/min; Scott and Williams drive.

UNCLASSIFIED
PHOTO 32926

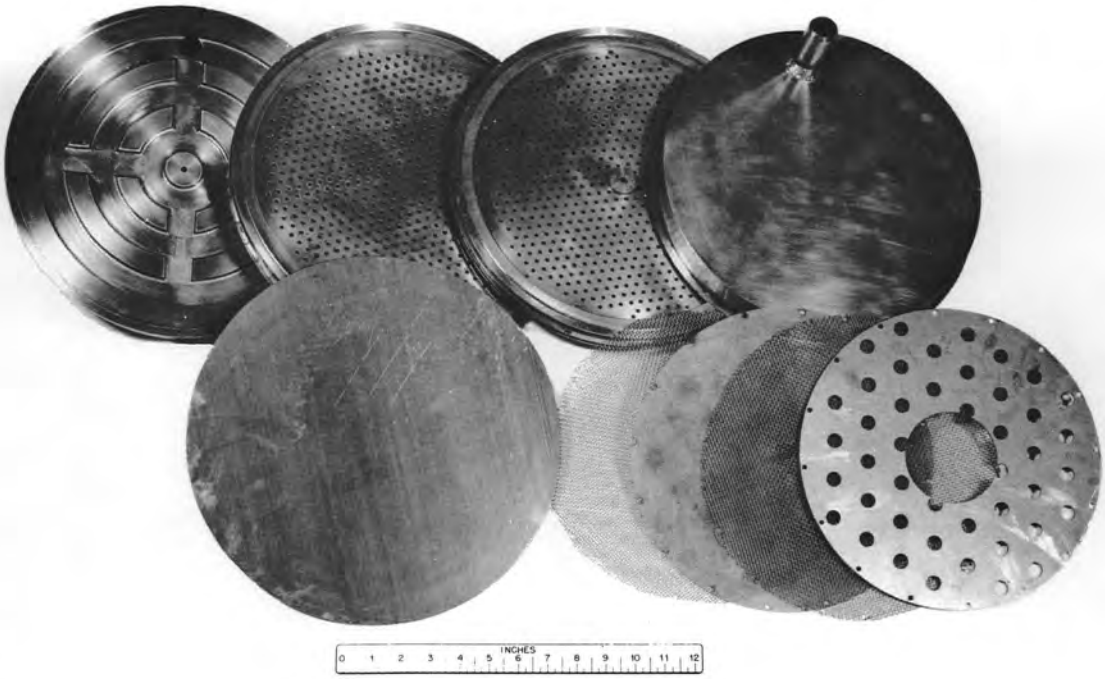

Fig. 24. Unassembled Experimental Diaphragm Pump Head.

of stainless steel diaphragms are initiated by deep scratches or indentations, presumably because of high stress concentrations. Further laboratory and service tests are planned to explore the hardenable alloys and titanium.

Since the difference between the endurance limit in air and that in fuel solution is believed to be due to corrosion and since in the tests 10^7 cycles were made in about four days, it is concluded that in all cases where the endurance was markedly reduced in fuel solution, the material is unsatisfactory for diaphragm use with fuel solution. Thus, although fully hard type 347 stainless steel appears (Table 3) to have a higher endurance limit than annealed type 347, the fully hard material has apparently lost more than half its endurance in air by immersion for four days in fuel solution, whereas the annealed material lost very little endurance in fuel solution, and the fully annealed material can be expected to provide longer diaphragm life.

The data in Table 3 are largely for comparison and cannot safely be used directly as a permissible combined stress. As mentioned in Sec 3.1.2, the choice of an allowable combined stress is made on the basis of experience, knowledge of the conditions under which the diaphragm will operate, and the endurance limits in air or inert fluid and in the fluid which is to be pumped.

Currently, reactor fuel pumps are designed for a combined stress of about 20,000 psi in mirror-finished, fully annealed type 347 stainless steel diaphragms, while the water pumps are designed for a combined stress of about 28,000 psi with the same material.

Table 3. Stresses (in psi) at Which Various Materials Will Endure 10^7 Cycles[a]

Material	In Air at Room Temp	In Distilled Water at 60°C	In Fuel Soln at 60°C	Elongation (%)
347 stainless steel				
Annealed	35,000[b]		34,000[c]	42
¼ hard	58,000[b]	50,000[b]	30,000	14
½ hard	67,000	57,000	31,000	2.5
¾ hard	88,000[b]		32,000	2.5
Full hard			43,000	2.5
316L stainless steel				
¼ hard			32,000	14[b]
½ hard			32,500	10[b]
AM-350 SBT[d]	90,000[b]	62,000	39,000	11[b]
Titanium 110 AT	70,000[b]	62,500	62,500	10[b]
CD 4M-Cu[e]			42,000	16

[a]F. H. Beck, *Fatigue and Corrosion Fatigue of Stainless Steel by Uranyl Sulphate*, Engineering Experiment Station, Ohio State University, Columbus, Ohio (Nov. 20, 1959).

[b]Data taken from literature.

[c]More recent, and as yet incomplete, tests indicate an endurance limit of 28,000 psi or less for annealed type 347 stainless steel at 10^8 cycles in fuel solution. This agrees with other corrosion-fatigue work showing that in a corrosive environment the endurance limit is not asymptotic but continues to decrease with an increase in cycles.

[d]SBT refers to tempering by refrigeration followed by aging at 650°F.

[e]CD 4M-Cu is a ferritic alloy, developed at Ohio State University, which is hardenable by cold rolling and aging.

3.2 Exclusion of Solids from Pump Cavity

Since a diaphragm presses against part or all of the restraining contours during each stroke, hard particles can damage the diaphragm and cause failure either directly or as a result of stress concentrations in the vicinity of the damage. In addition, any appreciable accumulation of solids can alter the contour of the diaphragm and produce stresses which are greater than those predicted in the design. Hence it has been found desirable to minimize the movement of solids into the pump cavity by means of a screen arranged as shown in Fig. 1.

Figure 2 is a photograph of a disassembled head, with the screen tube shown in the foreground. It fits in a hole bored through the head flange and communicates with the pump chamber through the triple row of holes seen in the contour face of the head flange on the left. Prototype heads have evolved from no screening through 40 and 100 mesh, with a marked increase in life accompanying each reduction in mesh size. Experimental pumps have been operated with Poroloy filters of 40- and 20-μ rating with no apparent loss of efficiency. Poroloy filters,

which are more rigid than screens and are comparable in cost, are expected to eliminate the possibility of mechanical damage to the diaphragm; they will be specified for future units.

The required screen area for a given pump may be determined on the basis of permissible head loss, pump flow, and head loss per unit area of the filter material. Bench tests made on 11-in.-long Poroloy tubes, 0.75-in. ID by 0.032-in. wall, indicated a pressure drop of approximately 3 in. of water per gpm for a 20-μ-pore tube and approximately 0.6 in. of water per gpm for a 40-μ-pore tube.

3.3 Seal Welding

To assure complete containment, the diaphragm is seal-welded to both head flanges. A seal-weld lip $\frac{1}{16}$ in. thick and $\frac{1}{4}$ in. wide is machined on each head flange, a diaphragm with a diameter $\frac{1}{16}$ in. greater than the outside diameter of the seal-weld lip is clamped in position between the flanges, and the two lips and diaphragm are fused together. Diaphragms that have been seal-welded in pumps and then cut out, either before or after operation, exhibit a pronounced "oil can" effect; that is, they are dished about $\frac{1}{8}$ in. deep.

In order to determine whether diaphragms in head assemblies are dished so that they must "pop through" on every stroke and to determine the magnitude of the stresses induced by seal-welding, a series of test welds[12] were made on mock pump heads with 0.019-in.-thick type 347 annealed sheet diaphragms arranged in four cases for dial-indicator readings and in one case for strain-gage readings. Figure 25 shows a diagram of a seal-weld test flange having a recess rather than a contour and having holes for dial-indicator readings of the diaphragm position. Figure 26 shows the arrangement of strain gages on a test diaphragm. A contour plot was made of a diaphragm after it was clamped in place (Fig. 27) and again after it was seal-welded (Fig. 28). The strain-gage readings taken for radial and circumferential stresses of a diaphragm unrestrained, clamped, welded, and cut free (Figs. 29 and 30), show that although the diaphragms were cut from what would be considered a good, flat sheet stock, they were bowed after being clamped between the head flanges, and distortion stresses resulted. The seal-welding operation reduced the bowing and the stresses. Removing the diaphragm from the head, thereby removing the restraint provided by the head, permitted the outer weld-affected zone to shrink, which created the typical dish and increased the circumferential compressive stress and the radial tensile stress. Cutting off a $\frac{3}{4}$-in.-wide band removed most of the yielded metal, leaving the diaphragm nearly flat and reducing the net stress. As can be seen in Figs. 25 and 26, and as is the case in actual pump heads, the weld-affected zone is within the clamped area and does not flex.

It was concluded that the diaphragms in the heads are not dished and can be seal-welded without damage. The residual stresses after welding are small; in fact, the welding reduces the stresses and bowing introduced by clamping the irregular sheet-metal diaphragm. The recommended seal-weld procedure is to clamp the head flanges and diaphragm securely, make

[12] E. C. Hise, *Stresses and Deflections Induced in Seal Welding a Diaphragm Pump*, ORNL CF-57-9-55 (Sept. 18, 1957).

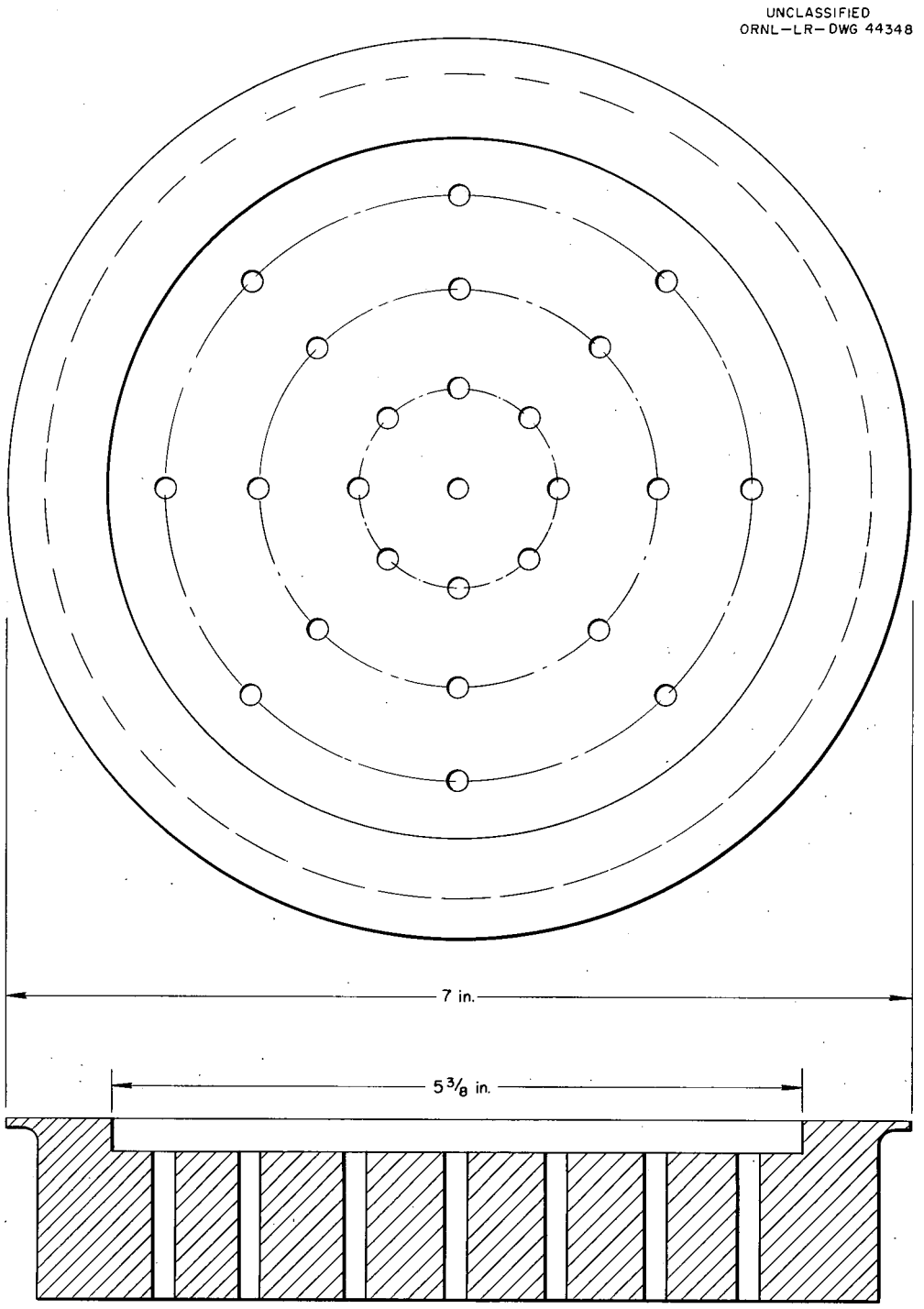

Fig. 25. Diagram of a Seal-Weld Test Head.

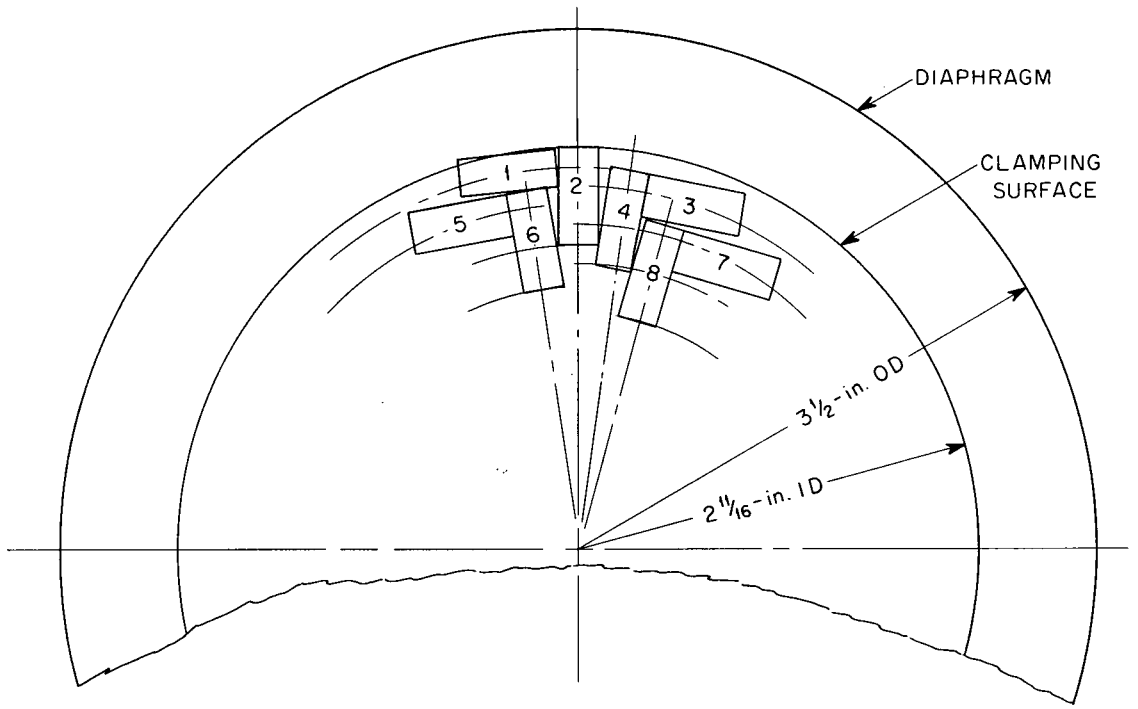

Fig. 26. Seal-Weld-Test Strain-Gage Location; Mirror Image on Reverse Side. Diaphragm material, 0.019-in.-thick type 347 stainless steel.

four tack welds at 90° intervals, and weld each segment in sequence. The sheet metal used for diaphragm stock should be as flat as obtainable, should be handled and cut in such a fashion as to maintain flatness, and should be deburred after cutting.

3.4 Pressure-Head Construction

Application of diaphragm pumps in reactor systems requires the pumps to withstand radiation, a corrosive environment, and severe pressure cycling. At present, radiation and corrosion resistance is obtained by constructing the units entirely of type 347 stainless steel, and integrity of the assembly is obtained by massive all-welded construction. In operation, failures have occurred at the joint of the pipe to the head flange (feed-pump heads 6 and 11, Table 4) as a result of the discontinuity stresses at this point. The tapered transition piece has corrected that problem; however, there have since been failures in the butt-welded joints of ¼-in. and ¾-in. sched-80 pipe after some 30 million cycles. It has become apparent that normal design criteria are not adequate where long-term pressure cycling is expected, and all components are being strengthened accordingly. Prototype HRT units have now been operated for two years and are still in operation, demonstrating the soundness of the design illustrated in Figs. 1 and 2.

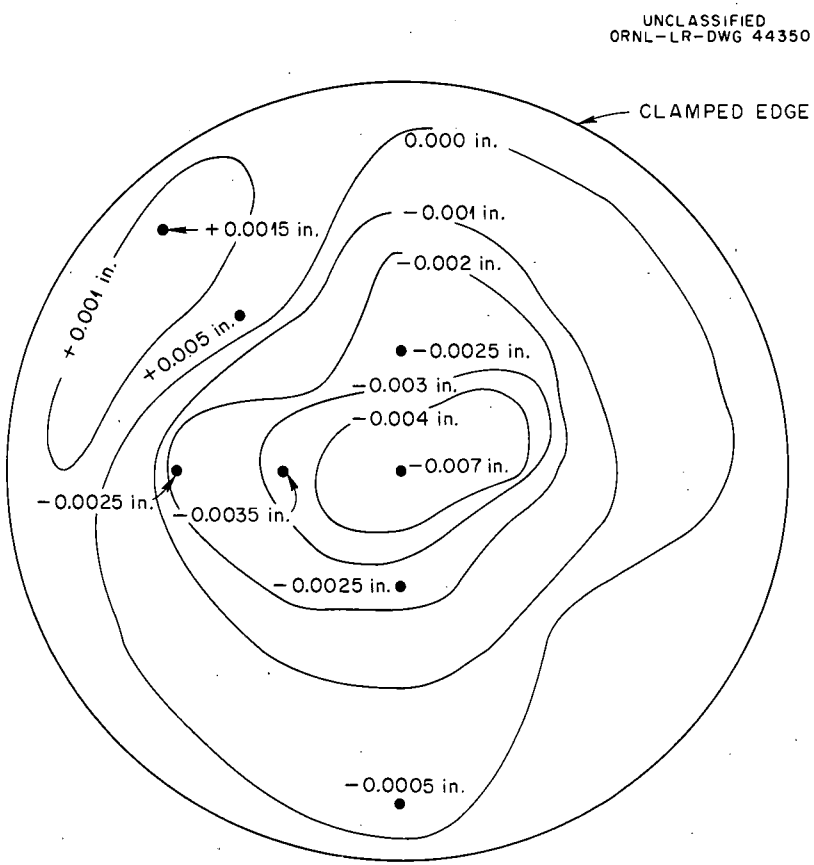

Fig. 27. Contour Plot of Diaphragm Clamped Between Test Heads Before Welding.

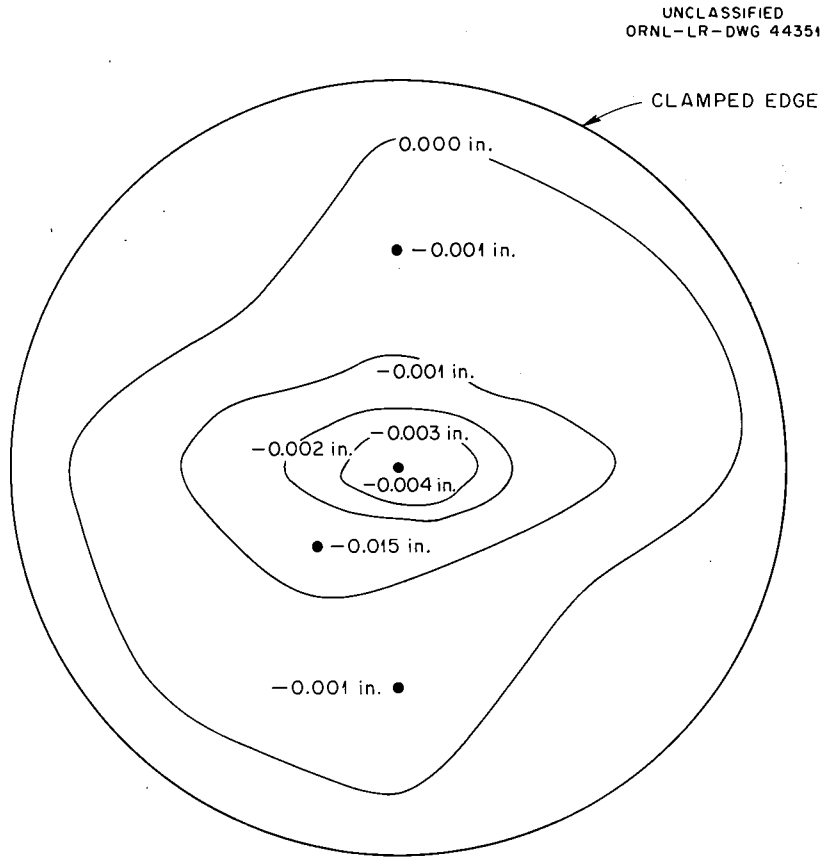

Fig. 28. Contour Plot of Diaphragm After Welding Between Test Heads.

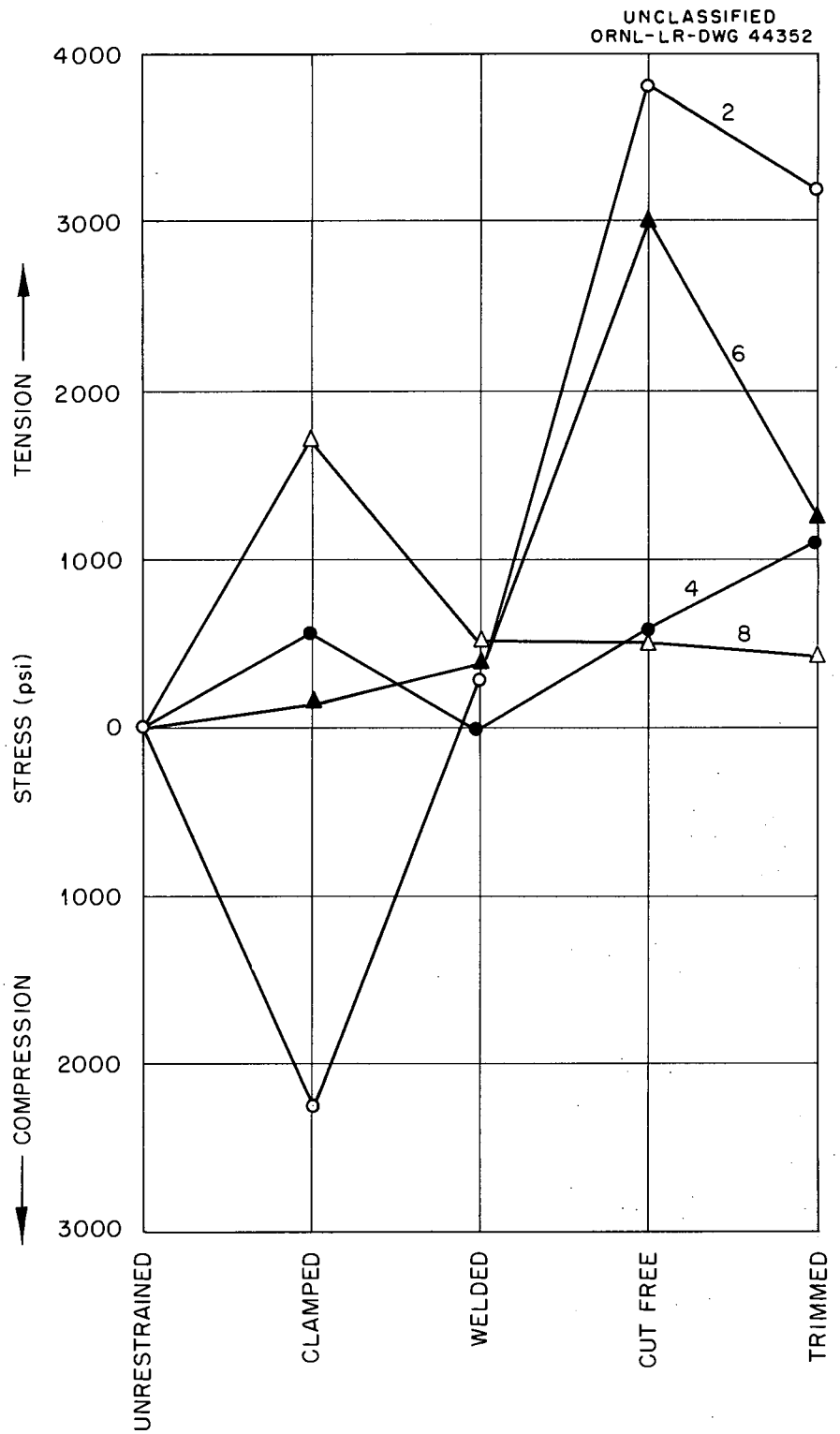

Fig. 29. Net Radial Stresses in Test Diaphragm.

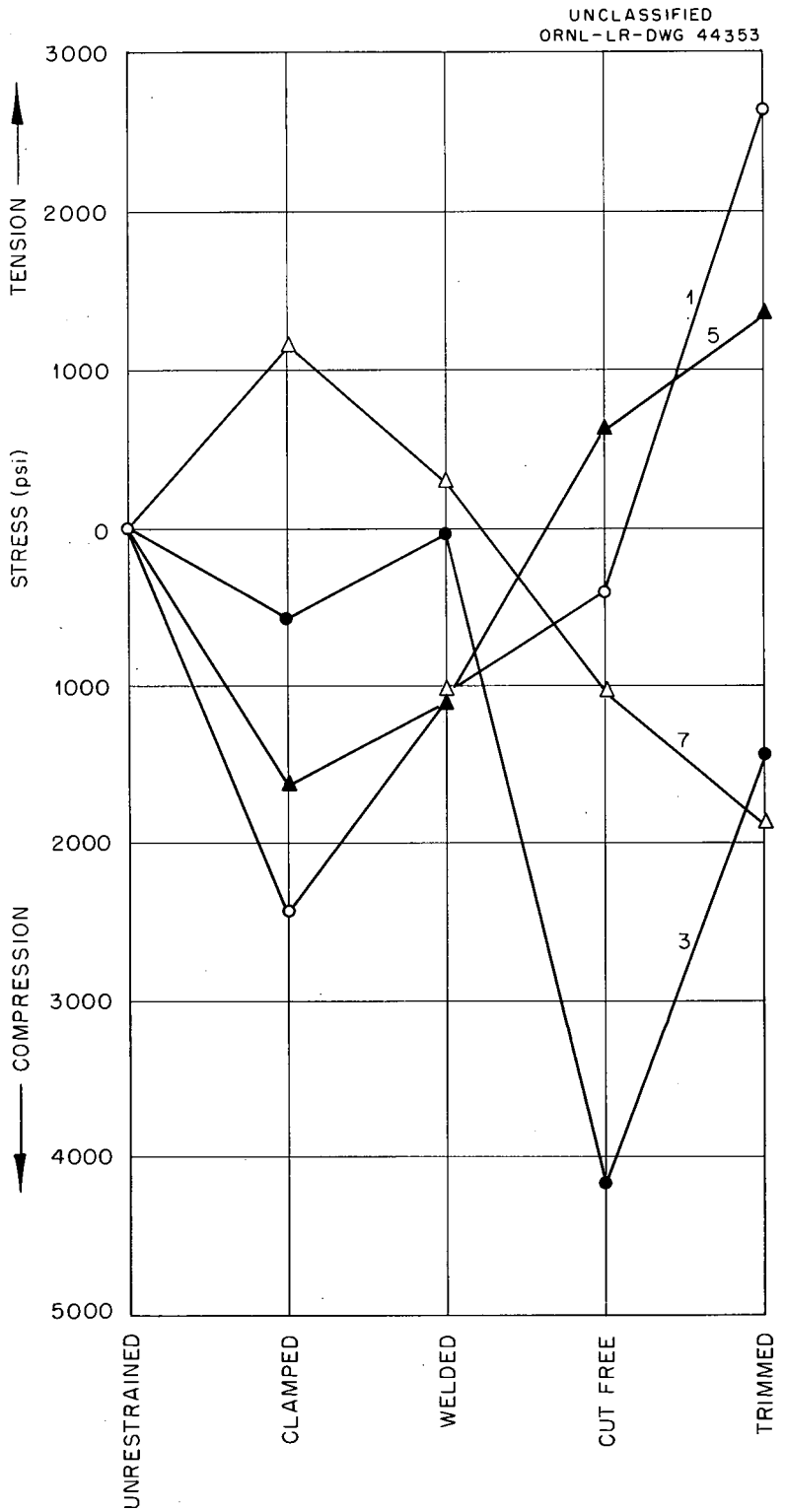

Fig. 30. Net Circumferential Stresses in Test Diaphragm.

4. CHECK VALVES

The development of high-integrity long-lived check valves has required consideration of the configuration, size, materials, and containment.

4.1 Configuration and Size

The double-ball gravity-operated check valve was chosen for HRT service for several reasons. Gravity operation eliminates springs and reduces the number of operating parts to a minimum. High-precision balls are readily available in any material that could be considered suitable for check-valve trim, whereas other types of plugs would be difficult to fabricate from materials such as ceramics. A ball plug needs guiding only for dynamic stability. It cannot be misaligned and will form a line-contact seal with a conical seat regardless of the position in which it happens to fall. Two balls in series are used to reduce the possibility of leakage and trim erosion in the event a foreign particle should hold one ball off its seat.

The original HRE valves (Fig. 31*a*) were adapted from commercial valves and operated satisfactorily except for a tendency to slam under certain conditions. This appeared to be the result of a delayed seating of the ball accompanied by water hammer, loud noise, and vibration of the associated piping severe enough to break a piece of ¼-in. sched-80 pipe in 4 hr on two occasions. The original valves had a 1-in. ball, a 0.625-in.-ID seat, a 0.125-in. ball-to-cage

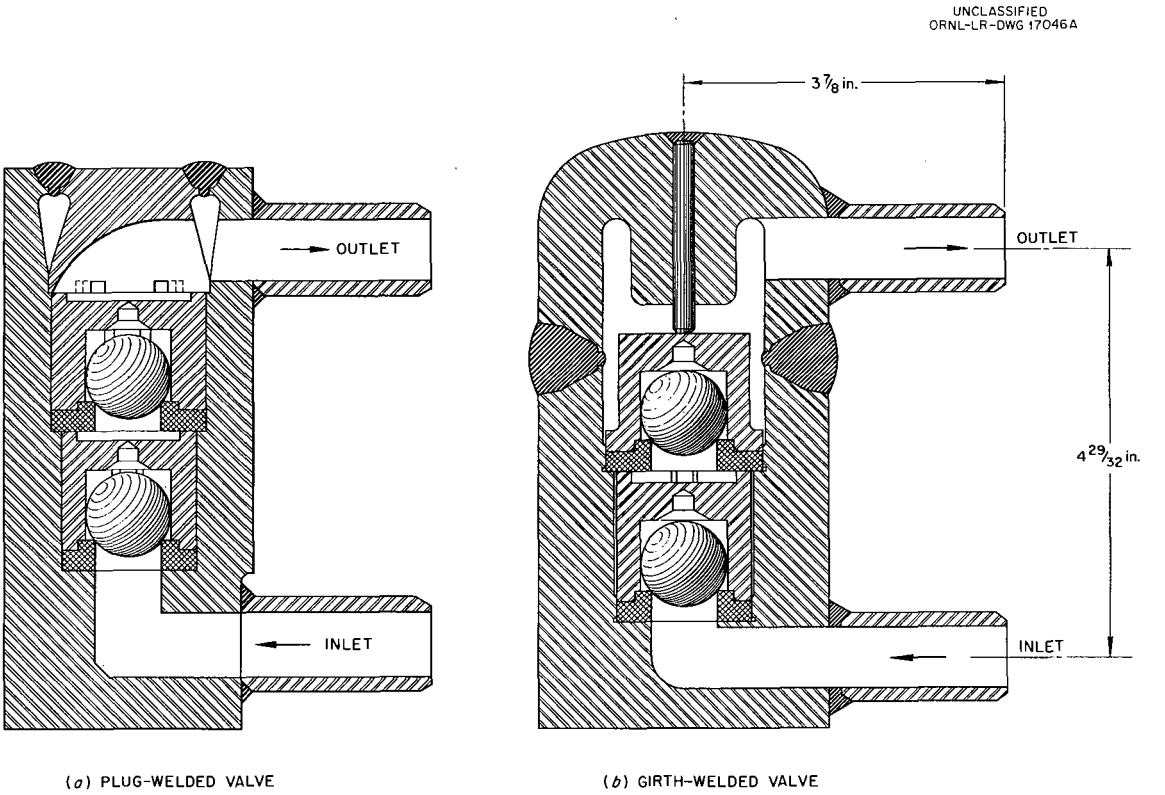

Fig. 31. (*a*) Plug-Welded Check Valve; (*b*) Girth-Welded Check Valve.

diametral clearance, and a lift of $\frac{5}{16}$ in. Progressive modifications have resulted in a valve having a 1-in. ball, an 0.812-in.-ID seat, a 0.010-in. ball-to-cage diametral clearance, and a 0.100-in. lift. The resulting valve has been tested at speeds up to 80 strokes/min and flows up to 2.9 gpm per unit; it has performed quietly and satisfactorily.

Where relatively clean fluids can be expected, close diametral guiding is advantageous; however, where the possibility of dirt exists or where slurries are to be pumped, the balls will stick in the cages. The dome-guide cage (Fig. 32) gives low lift and close guiding without the possibility of sticking. The ball rises into four spherical triangle segments, which permit little diametral movement. This design has been operated successfully for several thousand hours in solutions and slurries at speeds up to 100 strokes/min. It rattles more than the former design but appears to suffer no resultant instabilities or damage.

The HRT purge-pump valves use a 0.625-in. ball on a 0.535-in. seat and operate over a range of 0 to 0.4 gpm. These conditions give maximum velocities through the trim annulus up to 10 fps. At velocities of 2 to 5 fps the ball dances, as evidenced by a mild rattle, but at higher velocities it opens and closes firmly. The ball and seat dimensions represent adaptations of commercial practice. The ball-to-seat diameter ratio is fairly close to the American Petroleum Institute (API) standard.

An extensive literature search revealed no design data regarding the sizing of trim, desirable velocities, or ball-to-seat ratios. The API standards, however, provide a proved and satisfactory ball-to-seat ratio, and API standard balls and seats are available commercially in a variety of materials. The sizing of the valve can follow commercial practice, with modifications where necessary to adapt to special conditions of viscosity, suction head, etc.

4.2 Materials

The selection of trim material is dependent upon the fluid being pumped and the economics of trim replacement. It cannot be assumed that because a trim material is satisfactory in one corrosive fluid it will be satisfactory in a seemingly less corrosive fluid. The original HRT valves had Stellite Star J balls and Stellite No. 6 seats. These materials had been tested for thousands of operating hours in fuel solution with no evidence of leakage, corrosion, or erosion. However, during the precritical testing of the HRT system the seats failed in a few hundred hours of operation in distilled water. A series of dynamic check-valve material tests[13,14] were made to confirm this phenomenon and to select a more suitable seat material. It appeared that if the Stellite 6 seats were lapped to a perfect seal or first operated in fuel solution, they would operate satisfactorily in distilled water, but without either of these pretreatments they would fail from "wire drawing" in less than 200 hr. Stellite No. 3 and 17-4 PH stainless steel

---

[13] R. Blumberg, *Evaluation of Check Valve Materials in Uranyl Sulfate and in Distilled Water*, ORNL CF-57-12-72 (Dec. 17, 1957).

[14] R. Blumberg, *Further Evaluation of Check Valve Material for the Homogeneous Reactor Program*, ORNL CF-59-8-135 (Aug. 4, 1959).

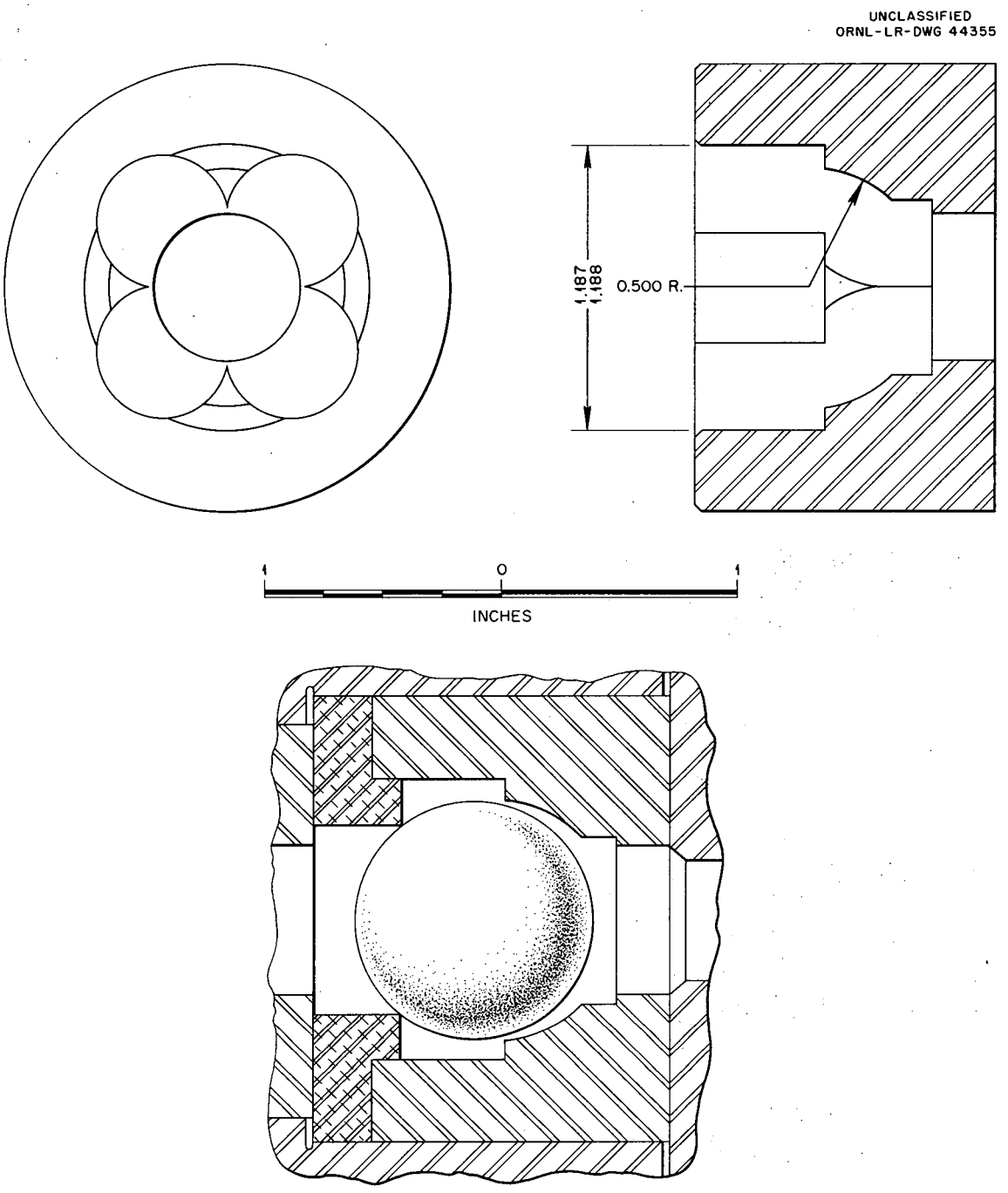

Fig. 32. Dome Guide Cage for 1-in. Ball.

hardened to R_C 40 were tested satisfactorily in water and in fuel solution for over 1000 hr. These materials have subsequently been in operation for over 10,000 hr both in water and in fuel solution. Type 347 and Carpenter 20 stainless steel seats appeared satisfactory in water during a 300-hr test. Platinum-bonded tungsten carbide (Kennametal K-501) and aluminum oxide appeared questionable or unsatisfactory on the basis of flow loss or weight loss in water or fuel solution.

It was demonstrated that even seemingly similar materials will give vastly different service and that the selection of check-valve trim material must be made on the basis of experience with the material in its specific intended application or applications. The materials recommended for the HRT feed and purge pumps on the basis of these tests are Stellite Star J balls and Stellite No. 3 or type 17-4 PH stainless steel seats.

4.3 Containment

For reactor use where absolute containment is necessary and trim replacement is impractical, a welded assembly is mandatory. The HRE check valves, which were designed for 1000-psi operation, used a plug-weld closure (Fig. 31*a*). When this valve was tested at 2000 psi for HRT application, the plug welds cracked through after three to four million cycles. The design was changed to the girth-weld closure (Fig. 31*b*) and has suffered no failures after 70 million cycles.

For out-of-pile use where maintenance is possible and experimental trim replacement is desirable, a bolted-and-gasketed assembly is used.

The degree of containment should be consistent with the application, but where long life is desired the design must take into account the cyclic stress nature of check-valve service and contain no fatigue stress risers.

It is of importance to note that the suction check-valve assembly is subjected to continual pressure cycling between the suction and discharge pressure, whereas the discharge valve assembly is subjected only to the discharge pressure.

5. OPERATING HISTORY OF HEADS AND VALVES

The operating history from 1955 to April 1959 of prototype and HRT feed- and purge-pump heads and check valves is recorded in Tables 4–7. Some of these units were life-tested and were therefore operated to destruction. Others were operated as auxiliaries to test systems and to the HRT, in which cases they may have been removed from service for reasons other than failure. The units removed from the HRT after October 1957 were contaminated and were not examined. The cause of failure listed for such units was deduced from the operating characteristics, pressure-time traces, or presence of radioactivity in the intermediate system.

The unit replacement design typified by Fig. 3 has proved to be very satisfactory. Three feed-pump heads and two purge-pump heads have been replaced by completely remote methods

Table 4. Operating History of Feed-Pump Heads

Head Number	Operating Location	Date Installed	Date Removed	Hours of Operation	Diaphragm	Screen	Pumped Fluid	Type of Assembly	Remarks
Unnumbered	HRT mockup	Unknown	Unknown	2,800	0.019 in., 347 SS, full anneal	40 mesh	Depleted fuel	Welded	Branched crack in lower portion of diaphragm; many dents
1	HRT mockup, south	Early 1955	2-7-56	3,298	0.019 in., 347 SS, full anneal, brush finish	40 mesh	Depleted fuel	Welded	Circumferential crack 1½ in. long in lower portion of diaphragm; several smaller cracks and many dents
1	HRT mockup, south	3-22-56	4-24-56	488	0.019 in., A-40 titanium, pickled finish	40 mesh	Depleted fuel	Bolted	Large circumferential crack; method of assembly and materials used rendered test inconclusive
2	Feed-pump test loop No. 1, west	2-15-56	1-16-58	9,000	0.019 in., 347 SS, full anneal, brush finish	40 mesh	Water	Welded	Circumferential crack in lower diaphragm; head had operated an unknown number of hours prior to installation on FPTL No. 1; 9000 hr accumulated on FPTL No. 1
3	HRT mockup, north	3-3-56	2-16-57	6,757	0.019 in., 347 SS, full anneal, brush finish	40 mesh	Depleted fuel	Welded	Branched crack near bottom of diaphragm; dents
5	Feed-pump test loop No. 1, east	4-3-57	9-10-57	2,194	0.031 in., 347 SS, full anneal, liquid-blast finish	40 mesh	Water	Bolted	Removed from service; no failure
6	HRT mockup, south	8-14-56	12-17-58	12,875	0.022 in., 347 SS, ¼ hard, mechanically polished	40 mesh	Depleted fuel	Welded	Blanked-off lower nipple cracked at 2408 hr; nipple was removed; hole was plugged; and head continued in service to diaphragm failure at 12,875 hr
7	Valve test loop	11-30-56	6-17-57	1,103	0.027 in., 347 SS, ¼ hard, mechanically polished	40 mesh	Depleted fuel	Bolted	2¼-in. crack near bottom; heavily indented
9	Feed-pump test loop No. 2, south	2-7-57		16,300	0.031 in., 347 SS, full anneal, mirror finish	100 mesh	Fuel	Welded	In operation
10	Feed-pump test loop No. 2, north	2-7-57		16,300	0.031 in., 347 SS, full anneal, mirror finish	100 mesh	Depleted fuel	Welded	In operation
11	HRT mockup, north	3-27-57	9-6-57	1,799	0.031 in., 347 SS, ½ hard, stress relieved	100 mesh	Depleted fuel	Bolted and seal-welded	Blanked intermediate nipple cracked at 1100 hr; nipple removed and hole plugged; seal weld cracked at 1799 hr; probably result of handling during previous repair

Table 4 (continued)

Head Number	Operating Location	Date Installed	Date Removed	Hours of Operation	Diaphragm	Screen	Pumped Fluid	Type of Assembly	Remarks
12	Multipump loop	11-8-57		7,791	Two, 0.031 in., 347 SS, full anneal, mirror finish	100 mesh	Depleted fuel	Bolted and seal-welded	In operation; double-diaphragm—double-capacity pump
13	HRT mockup, north	9-11-57		8,996	0.031 in., 347 SS, full anneal, mirror finish	100 mesh	Depleted fuel	Welded	In operation
14	Valve test loop	12-27-57		2,857	0.031 in., 347 SS, full anneal, mirror finish	20 μ	Depleted fuel	Bolted	In operation
16	HRT mockup, south	2-13-59		723	0.031 in., 347 SS, full anneal, mirror finish	100 mesh	Depleted fuel	Welded	In operation
21	Multipump loop	11-12-58		2,595	0.031 in., 347 SS, full anneal, mirror finish	20 μ	Depleted fuel	Bolted	In operation; 12-in.-dia 0.125-in.-deep free-deflection contour
HRT Feed-Pump Heads									
HRT 3	Blanket feed, east	10-11-56	4-2-57	2,341	0.019 in., 347 SS, full anneal, brush finish	40 mesh	Water	Welded	No failure
HRT 5	Fuel feed, west	1-21-57	2-26-57	496	0.019 in., 347 SS, full anneal, brush finish	40 mesh	Water and depleted fuel	Welded	Check valves leaked
HRT 6	Fuel feed, west	10-11-56	1-21-57	1,029	0.019 in., 347 SS, full anneal, brush finish	40 mesh	Water and depleted fuel	Welded	Check valves leaked and were replaced
HRT 6	Fuel feed, west	2-26-57	10-1-57	707	0.019 in., 347 SS, full anneal, brush finish	40 mesh	Water and depleted fuel	Welded	No failure
HRT 6	Fuel feed, east	8-9-57	10-1-57	317	0.019 in., 347 SS, full anneal, brush finish	40 mesh	Water and depleted fuel	Welded	No failure; diaphragm operated total 2053 hr
HRT 7	Fuel feed, east	10-11-56	2-26-57	1,525	0.019 in., 347 SS, full anneal, brush finish	40 mesh	Water and depleted fuel	Welded	Suction check failed at 1029 hr; both valves failed at 1525 hr and were replaced
HRT 7	Blanket feed, east	8-9-57	10-1-57	150	0.019 in., 347 SS, full anneal, brush finish	40 mesh	Water	Welded	No failure; 1674 hr total
HRT 8	Blanket feed, west	2-20-57	10-1-57	958	0.019 in., 347 SS, full anneal, brush finish	40 mesh	Water	Welded	No failure
HRT 9	Fuel feed, east	2-26-57	4-2-57	706	0.019 in., 347 SS, full anneal, brush finish	40 mesh	Water and depleted fuel	Welded	No failure
HRT 9	Fuel feed, west	8-9-57	10-1-57	317	0.019 in., 347 SS, full anneal, brush finish	40 mesh	Water and depleted fuel	Welded	No failure; 1023 hr total

Table 4 (continued)

Head Number	Operating Location	Date Installed	Date Removed	Hours of Operation	Diaphragm	Screen	Pumped Fluid	Type of Assembly	Remarks
HRT Feed-Pump Heads									
HRT 12	Blanket feed, west	10-11-56	2-20-57	1,530	0.019 in., 347 SS, full anneal, brush finish	40 mesh	Water	Welded	No failure
HRT 13	Blanket feed, east	10-25-57		3,688	0.031 in., 347 SS, full anneal, mirror finish	100 mesh	Water and fuel	Welded	In operation
HRT 14	Blanket feed, west	10-1-57		3,688	0.031 in., 347 SS, full anneal, mirror finish	100 mesh	Water and fuel	Welded	In operation
HRT 15	Fuel feed, east	10-1-57	7-26-58	2,283	0.031 in., 347 SS, full anneal, mirror finish	100 mesh	Fuel	Welded	Reading of 10 mr/hr on intermediate pipe; reading decreased with time; no other indications of foilure; head removed as precautionary measure
HRT 16	Fuel feed, west	10-1-57	4-29-59	5,000	0.031 in., 347 SS, full anneal, mirror finish	100 mesh	Fuel	Welded	Lost intermediate woter while in operation; no leakage apparent on 2500-psi hydrostatic test
HRT 21	Fuel feed, east	7-26-58	2-13-59	2,278	0.031 in., 347 SS, full anneal, mirror finish	100 mesh	Fuel	Welded	Reading 10 r/hr on intermediate water; other indications of diaphragm rupture
HRT 22	Fuel feed, west	4-29-59		7	0.031 in., 347 SS, full anneal, mirror finish	100 mesh	Fuel	Welded	In operation
HRT 23	Fuel feed, east	2-13-59		39	0.031 in., 347 SS, full anneal, mirror finish	100 mesh	Fuel	Welded	In operation

Table 5. Operating History of Feed-Pump Check Valves

Type and No.	Operating Location	Head No.	Date Installed	Date Removed	Hours of Operation	Seat Material	Ball Material	Type of Assembly	Pumped Fluid	Remarks
Suction, unnumbered	HRT mockup		8-8-55	10-14-55	718	Stellite 6	Star J	Plug weld	Depleted fuel	Crack originating in root of closure weld and terminating in top of housing between closure weld and outer edge
Suction, unnumbered	HRT mockup		10-16-55	1-30-56	1,286	Stellite 6	Star J	Plug weld	Depleted fuel	
D-1	HRT mockup and feed-pump test No. 1		4-2-56	5-22-57	5,767	Stellite 6	Star J	Girth weld	Depleted fuel and water	Removed from service in good condition
D-2	Feed-pump test No. 1		2-15-56	1-16-58	8,975	Stellite 6	Star J	Girth weld	Water	Removed from service in good condition
D-3	HRT mockup		3-1-56	11-15-56	5,768	Stellite 6	Star J	Girth weld	Depleted fuel	Removed from service in good condition
D-4	Feed-pump test No. 1		1-15-56	9-5-56	962	Stellite 6	Star J	Girth weld	Water	Leakage through trim
D-5	Feed-pump test No. 1		9-10-56	10-22-56	732	Stellite 6	Star J	Girth weld	Water	Leakage through trim
D-6	Feed-pump test No. 1		11-1-56	5-11-57	763	Stellite 6	Star J	Girth weld	Water	Removed from service in good condition
D-7	Feed-pump test No. 2		10-22-56	12-10-56	563	Stellite 6	Star J	Girth weld	Water	Trim leaked badly
D-8	Feed-pump test No. 2		10-22-56	12-10-56	563	Stellite 6	Star J	Girth weld	Water	Satisfactory
D-8	HRT mockup		3-11-57		11,999	Stellite 6	Star J	Girth weld	Depleted fuel	In operation
D-9	HRT mockup		11-5-56		11,552	Stellite 6	Star J	Girth weld	Depleted fuel	In operation
D-10	HRT mockup		11-5-56		11,919	Stellite 6	Star J	Girth weld	Depleted fuel	In operation
D-11	Valve test loop		12-19-56	2-19-58	2,896	Stellite 3	Star J	Girth weld	Depleted fuel	Exact history and operating hours unknown; salvaged because it was plug-weld design
D-12	Feed-pump test No. 2		1-23-56		16,300	Stellite 6	Star J	Girth weld	Depleted fuel	In operation

Table 5 (continued)

Type and No.	Operating Location	Head No.	Date Installed	Date Removed	Hours of Operation	Seat Material	Ball Material	Type of Assembly	Pumped Fluid	Remarks
D-13	Feed-pump test No. 2		1-23-56	10-8-58	5,239	Stellite 6	Star J	Girth weld	Depleted fuel	Removed from service in good condition to test D-14
D-14	Feed-pump test No. 2		2-19-57		13,918	17-4 PH	Haynes 25	Girth weld	Depleted fuel	In operation
D-15	Multipump loop		11-8-57		7,217	Stellite 3	Star J	Girth weld	Depleted fuel	In operation
S-1	HRT mockup		3-23-56		15,885	Stellite 6	Star J	Girth weld	Depleted fuel	In operation; contains trim salvaged from earlier valve-history unknown
S-2	Feed-pump test No. 1		4-19-56	1-22-58	8,400	Stellite 6	Star J	Girth weld	Water	Removed from service in good condition; contains salvaged trim
S-3	HRT mockup		3-23-56		17,007	Stellite 6	Star J	Girth weld	Depleted fuel	In operation; contains salvoged trim
S-4	Feed-pump test No. 1		4-19-56	12-13-56	1,714	Stellite 6	Star J	Girth weld	Water	Removed from service in good condition; contains salvaged trim
S-5	Feed-pump test No. 1		10-22-56	6-5-57	2,420	Stellite 6	Star J	Girth weld	Water	Severe leakage
S-6	Feed-pump test No. 2		10-22-56	12-10-56	563	Stellite 6	Star J	Girth weld	Water	Leaks
S-7	Valve test loop		12-4-56	1-22-58	2,916	Stellite 6	Star J	Girth weld	Depleted fuel	Removed from service in good condition
S-8	Feed-pump test No. 2		2-7-57		16,300	Stellite 6	Star J	Girth weld	Depleted fuel	In operation
S-9	Feed-pump test No. 2		3-21-57	10-8-58	5,239	Stellite 6	Star J	Girth weld	Depleted fuel	Leaks 2 cc/min at 2000 psi ΔP
S-10	Feed-pump test No. 1		6-5-57	8-22-57	1,024	17-4 PH	Star J	Girth weld	Water	Removed from service in good condition
S-11	Feed-pump test No. 2		7-19-57		13,918	17-4 PH	Star J	Girth weld	Depleted fuel	In operation
S-12	Multipump loop		11-8-57		7,217	Stellite 3	Star J	Girth weld	Depleted fuel	In operation

Table 5 (continued)

Type and No.	Operating Location	Head No.	Date Installed	Date Removed	Hours of Operation	Seat Material	Ball Material	Type of Assembly	Pumped Fluid	Remarks
HRT Feed-Pump Check Valves										
S, unknown	Blanket feed	3	10-11-56	4-2-57	2,341	Stellite 6	Star J	Girth weld	Water	No failure
D, unknown	Blanket feed	3	10-11-56	4-2-57	2,341	Stellite 6	Star J	Girth weld	Water	No failure
S, unknown	Fuel feed	5	1-21-57	2-26-57	496	Stellite 6	Star J	Girth weld	Water and depleted fuel	Removed because of leakage
D, unknown	Fuel feed	5	1-21-57	2-26-57	496	Stellite 6	Star J	Girth weld	Water and depleted fuel	Removed because of leakage
S, unknown	Fuel feed	6	10-11-56	1-21-57	1,029	Stellite 6	Star J	Girth weld	Water and depleted fuel	Removed because of leakage
D, unknown	Fuel feed	6	10-11-56	1-21-57	1,029	Stellite 6	Star J	Girth weld	Water and depleted fuel	Removed because of leakage
D-1	Fuel feed	6	2-26-57	10-1-57	1,024	Stellite 6	Star J	Girth weld	Water and depleted fuel	No failure
S-5	Fuel feed	6	2-26-57	10-1-57	1,024	Stellite 6	Star J	Girth weld	Water and depleted fuel	No failure
S, unknown	Fuel feed	7	10-11-56	1-21-57	1,029	Stellite 6	Star J	Girth weld	Water and depleted fuel	Removed because of leakage
S, unknown	Fuel feed	7	1-21-57	2-26-57	496	Stellite 6	Star J	Girth weld	Water and depleted fuel	Removed because of leakage
D, unknown	Fuel feed	7	10-11-56	2-26-57	1,525	Stellite 6	Star J	Girth weld	Water and depleted fuel	Removed because of leakage
S-3	Blanket feed	7	8-9-57	10-1-57	150	Stellite 6	Star J	Girth weld	Water	No failure
D-2	Blanket feed	7	8-9-57	10-1-57	150	Stellite 6	Star J	Girth weld	Water	No failure
S-7	Blanket feed	8	2-20-57	10-1-57	958	Stellite 6	Star J	Girth weld	Water	No failure
D-3	Blanket feed	8	2-20-57	10-1-57	958	Stellite 6	Star J	Girth weld	Water	No failure
S-6	Fuel feed	9	2-26-57	4-2-57	706	Stellite 6	Star J	Girth weld	Water and depleted fuel	No failure

Table 5 (continued)

Type and No.	Operating Location	Head No.	Date Installed	Date Removed	Hours of Operation	Seat Material	Ball Material	Type of Assembly	Pumped Fluid	Remarks
HRT Feed-Pump Check Valves										
S-4	Fuel feed	9	2-26-57	4-2-57	706	Stellite 6	Star J	Girth weld	Water and depleted fuel	No failure
S-6	Fuel feed	9	8-9-57	10-1-57	1,023 total	Stellite 6	Star J	Girth weld	Water and depleted fuel	No failure
D-4	Fuel feed	9	8-9-57	10-1-57	1,023 total	Stellite 6	Star J	Girth weld	Water and depleted fuel	No failure
S and D, unknown	Blanket feed	12	10-11-56	2-20-57	1,530	Stellite 6	Star J	Girth weld	Water	No failure
S-12	Blanket feed	13	10-25-57		3,688	17-4 PH	Star J	Girth weld	Water and fuel	In operation
D-12	Blanket feed	13	10-25-57		3,686	17-4 PH	Star J	Girth weld	Water and fuel	In operation
S-13	Blanket feed	14	10-1-57		3,688	17-4 PH	Star J	Girth weld	Water and fuel	In operation
D-13	Blanket feed	14	10-1-57		3,688	17-4 PH	Star J	Girth weld	Water and fuel	In operation
S-10	Fuel feed	15	10-1-57	7-26-59	2,283	Stellite 3	Star J	Girth weld	Fuel	Removed because of diaphragm failure; na valve failure indicated
D-10	Fuel feed	15	10-1-57	7-26-59	2,283	Stellite 3	Star J	Girth weld	Fuel	Removed because of diaphragm failure; no valve failure indicated
S-11	Fuel feed	16	10-1-57	4-29-59	5,000	Stellite 3	Star J	Girth weld	Fuel	No failure
D-11	Fuel feed	16	10-1-57	4-29-59	5,000	Stellite 3	Star J	Girth weld	Fuel	No failure
S-14	Fuel feed	21	7-26-58	2-13-59	2,278	Stellite 3	Star J	Girth weld	Fuel	Removed because of diaphragm failure; no valve failure indicated
D-14	Fuel feed	21	7-26-58	2-13-59	2,278	Stellite 3	Star J	Girth weld	Fuel	Removed because of diaphragm failure; no valve failure indicated
S-16	Fuel feed	23	2-13-59		39	Stellite 3	Star J	Girth weld	Fuel	In operation
D-17	Fuel feed	23	2-13-59		39	Stellite 3	Star J	Girth weld	Fuel	In operation
S-17	Fuel feed	22	4-29-59		7	Stellite 3	Star J	Girth weld	Fuel	In operation
D-16	Fuel feed	22	4-29-59		7	Stellite 3	Star J	Girth weld	Fuel	In operation

Table 6. Operating History of Purge-Pump Heads

Head Number	Operating Location	Date Installed	Date Removed	Hours of Operation	Diaphragm	Screen	Pumped Fluid	Type of Assembly	Remarks
Unnumbered	HRT mockup			2730	0.019 in., 347 SS, full anneal, brush finish	None	Water	Welded	Diaphragm crack started at large dent caused by metal particle found in head
P1	HRT mockup	6-20-56	4-4-57	4033	0.019 in., 347 SS, full anneal, brush finish	None	Water	Welded	$1\frac{3}{4}$-in.-long circular crack near bottom of diaphragm; many dents
P2	Purge-pump test 1	4-4-56	2-20-57	5732	0.019 in., 347 SS, full anneal, brush finish	None	Water	Welded	Circular crack originating in deep dent
P3	Purge-pump test 2	10-29-56	11-26-56	547	0.019 in., 347 SS, $\frac{1}{4}$ hard, polished	None	Water	Welded	Spectacular semicircular crack extending around entire bottom half
P4	HRT mockup	7-10-57		8620	0.019 in., 347 SS, full anneal, polished	100 mesh	Water	Welded	In operation
P5	Purge-pump test 2	8-30-57	10-10-58	8380	0.019 in., AM-350,[a] polished	100 mesh	Fuel	Welded	Test discontinued; operation was at 250 strokes/min
P6	Purge-pump test 1	8-30-57	10-10-58	8380	0.019 in., 347 SS, full hard, polished	100 mesh	Water	Welded	Test discontinued; operation was at 250 strokes/min
P11A	Purge-pump test 1	3-6-57	5-22-57	946	0.019 in., 347 SS, anneal[b]	None	Water	Welded	Diaphragm failed
P12A	HRT mockup	4-10-57	6-19-57	1298	0.019 in., 347 SS, anneal[b]	None	Water	Welded	Diaphragm failed
HRT Purge-Pump Heads[c]									
HRT 1	BCPPP[c]	10-11-56	4-2-57	1796	0.019 in., 347 SS, anneal[b]	None	Water	Welded	No failure; replaced during HRT flange replacement
HRT 4	FCPPP	10-11-56	4-2-57	1967	0.019 in., 347 SS, anneal[b]	None	Water	Welded	No failure; replaced during HRT flange replacement
HRT 4	FPPP	8-3-57	10-25-57	2508 total	0.019 in., 347 SS, anneal[b]	None	Water	Welded	Removed because of check-valve failure
HRT 5	FPPP	10-11-56	2-5-57	783	0.019 in., 347 SS, anneal[b]	None	Water	Welded	Broken diaphragm
HRT 6	BPPP	10-11-56	12-4-56	414	0.019 in., 347 SS, anneal[b]	None	Water	Welded	Leaking suction check

Table 6 (continued)

Head Number	Operating Location	Date Installed	Date Removed	Hours of Operation	Diaphragm	Screen	Pumped Fluid	Type of Assembly	Remarks
HRT Purge-Pump Heads[c]									
HRT 6	BPPP	8-3-57	10-25-57	470 total	0.019 in., 347 SS, anneal[b]	None	Water	Welded	No failure; replaced during flange replacement
HRT 7	FPPP	2-5-57	3-2-57	406	0.019 in., 347 SS, anneal[b]	None	Water	Welded	Broken diaphragm
HRT 8	BPPP	12-4-56	4-2-57	1383	0.019 in., 347 SS, anneal[b]	None	Water	Welded	No failure
HRT 8	FCPPP	8-3-57	10-25-57	1941 total	0.019 in., 347 SS, anneal[b]	None	Water	Welded	No failure
HRT 9	BCPPP	8-3-57	10-25-57	232	0.019 in., 347 SS, anneal[b]	None	Water	Welded	No failure
HRT 17	BCPPP	10-25-57		4656	0.019 in., 347 SS, full anneal, mirror finish	100 mesh	Water	Welded	In operation
HRT 18	FPPP	10-25-57		4754	0.019 in., 347 SS, full anneal, mirror finish	100 mesh	Water	Welded	In operation
HRT 19	BPPP	10-25-57	2-11-59	3654	0.019 in., 347 SS, full anneal, mirror finish	100 mesh	Water	Welded	Removed because of leaking suction check valve
HRT 20	FCPPP	10-25-57	2-13-59	4149	0.019 in., 345 SS, full anneal, mirror finish	100 mesh	Water	Welded	Removed because of leaking check valves
HRT 30	BPPP	2-11-59		216	0.019 in., 347 SS, full anneal, mirror finish	100 mesh	Water	Welded	In operation
HRT 31	FCPPP	2-13-59		405	0.019 in., 347 SS, full anneal, mirror finish	100 mesh	Water	Welded	In operation

[a]Heat treatment for AM-350: held at −100°F for 2 hr, then at 650°F for 2 hr.

[b]Diaphragms had been "polished" on lathe face plate with emery cloth, leaving circular scratches.

[c]BCPPP: blanket circulating-pump purge pump;
FCPPP: fuel circulating-pump purge pump;
BPPP: blanket pressurizer purge pump;
FPPP: fuel pressurizer purge pump.

Table 7. Operating History of Purge-Pump Check Valves

Check Valve Type and No.	Operating Location	Date Installed	Date Removed	Hours of Operation	Seat Material	Ball Material	Type of Assembly	Pumped Fluid	Remarks
S, unknown	HRT mockup	1-10-56	2-5-56	445	Stellite 6	Star J	Plug weld	Water	Crack originating in root of closure weld and terminating in side of housing $\frac{1}{8}$ in. from top
S, unknown	HRT mockup	2-7-56	2-26-56	398	Stellite 6	Star J	Plug weld	Water	Crack originating in root of closure weld and terminating in side of housing $\frac{1}{8}$ in. from top
S-1	HRT mockup	3-2-56	4-4-57	5,917	Stellite 6	Star J	Girth weld	Water	Removed from service; leak-tested and found not to leak
S-2	Purge-pump test loop 1		7-5-56	~3,000	Stellite 6	Star J	Girth weld	Water	Balls sticking in cages, seemingly from dirt
S-3	Purge-pump test 1	8-5-56	12-10-58	11,879	Stellite 6	Star J	Girth weld	Water	Test discontinued; leak-tested and found not to leak
S-4	Purge-pump test 2	10-29-56	11-26-56	547	Stellite 6	Star J	Girth weld	Water	Test discontinued
S-11	Purge-pump test 1	2-28-57	12-10-58	9,326	Stellite 6	Star J	Girth weld	Water	Test discontinued; static leak rate 1.29 cc/min at 2000 psi ΔP (used as discharge)
S-12	HRT mockup	4-4-57		9,927	Stellite 6	Star J	Girth weld	Water	Still in service
S-13	Purge-pump test 2	9-1-57	12-10-58	8,380	17-4 PH	Haynes 25	Girth weld	Fuel	Test discontinued; static leak rate 0.062 cc/min at 2000 psi ΔP
D-1	HRT mockup	6-19-56	4-4-57	4,133	Stellite 6	Star J	Plug weld	Water	Static leak rate 150 cc/hr at 2000 psi ΔP
D-2	Purge-pump test 1	unknown	4-8-57	9,049	17-4 PH	440 SS	Plug weld	Water	Test discontinued; static leak rate 0.062 cc/hr at 2000 psi ΔP
D-3	Purge-pump test 2	10-29-56	11-26-56	547	Stellite 6	Star J	Girth weld	Water	Test discontinued
D-12	HRT mockup	4-4-57		9,927	Stellite 6	Star J	Girth weld	Water	Still in service
D-13	Purge-pump test 2	9-1-57	12-10-58	8,380	17-4 PH	Star J	Girth weld	Fuel	Test discontinued; static leak rate 0.029 cc/min at 2000 psi ΔP
HRT Purge-Pump Check Valves*									
D-3	FCPPP Head No. 4	10-11-56	4-2-57	1,967	Stellite 6	Star J	Girth weld	Water	One of the valves failed
S-3	FCPPP Head No. 4	10-11-56	4-2-57	1,967	Stellite 6	Star J	Girth weld	Water	One of the valves failed
S, unknown	FPPP Head No. 5	10-11-56	2-5-57	783	Stellite 6	Star J	Girth weld	Water	Removed because of diaphragm failure

*BCPPP: blanket circulating-pump purge pump;
FCPPP: fuel circulating-pump purge pump;
BPPP: blanket pressurizer purge pump;
FPPP: fuel pressurizer purge pump.

Table 7 (continued)

Check Valve Type and No.	Operating Location	Date Installed	Date Removed	Hours of Operation	Seat Material	Ball Material	Type of Assembly	Pumped Fluid	Remarks
HRT Purge-Pump Check Valves*									
D, unknown	FPPP Head No. 5	10-11-56	2-5-57	783	Stellite 6	Star J	Girth weld	Water	Removed because of diophragm failure
S-1	BPPP Head No. 6	10-11-56	12-4-56	414	Stellite 6	Star J	Girth weld	Water	Removed because of leakage
S-7	BPPP Head No. 6	8-3-57	10-25-57	56	Stellite 6	Star J	Girth weld	Water	No failure
D-1	BPPP Head No. 6	10-11-56	10-25-57	470	Stellite 6	Star J	Girth weld	Water	No failure
S, unknown	FPPP Head No. 7	2-5-57	3-2-57	406	Stellite 6	Star J	Girth weld	Water	No failure
D, unknown	FPPP Head No. 7	2-5-57	3-2-57	406	Stellite 6	Star J	Girth weld	Water	No failure
S-8	BPPP and FCPPP Head No. 8	12-4-56	4-2-57	1,941 total	Stellite 6	Star J	Girth weld	Water	No failure
D-8		8-3-57	10-25-57		Stellite 6	Star J	Girth weld	Water	No failure
S-2	BCPPP Head No. 9	8-3-57	10-25-57	232	Stellite 6	Star J	Girth weld	Water	No failure
D-2	BCPPP Head No. 9	8-3-57	10-25-57	232	Stellite 6	Star J	Girth weld	Water	No failure
S and D, unknown	BCPPP Head No. 1	10-11-56	4-2-57	1,796	Stellite 6	Star J	Girth weld	Water	No failure
S-3	FPPP Head No. 4	8-3-57	10-25-57	2,508 total	Stellite 6	Star J	Girth weld	Water	Check-valve leakage
D-3	FPPP Head No. 4	8-3-57	10-25-57	2,508 total	Stellite 6	Star J	Girth weld	Water	Check-valve leakage
S-2**	BCPPP Head No. 17	10-25-57		4,656	17-4 PH	Star J	Girth weld	Water	Still in service
D-4	BCPPP Head No. 17	10-25-57		4,656	17-4 PH	Star J	Girth weld	Water	Still in service
S-3	FPPP Head No. 18	10-25-57		4,754	17-4 PH	Star J	Girth weld	Water	Still in service
D-2	FPPP Head No. 18	10-25-57		4,754	17-4 PH	Star J	Girth weld	Water	Still in service
S-3	BPPP Head No. 19	10-25-57	2-11-59	3,654	17-4 PH	Star J	Girth weld	Water	Removed because of leakage
D-4	BPPP Head No. 19	10-25-57	2-11-59	3,654	17-4 PH	Star J	Girth weld	Water	Operated satisfactorily
S-1	FCPPP Head No. 20	10-25-57	2-13-59	4,149	17-4 PH	Star J	Girth weld	Water	Suspected of leaking
D-1	FCPPP Head No. 20	10-25-57	2-13-59	4,149	17-4 PH	Star J	Girth weld	Water	Suspected of leaking
S-5	BPPP Head No. 30	2-11-59		210	17-4 PH	Star J	Girth weld	Water	Still in service
D-5	BPPP Head No. 30	2-11-59		210	17-4 PH	Star J	Girth weld	Water	Still in service
S-6	FCPPP Head No. 31	2-13-59		405	17-4 PH	Star J	Girth weld	Water	Still in service
D-6	FCPPP Head No. 31	2-13-59		405	17-4 PH	Star J	Girth weld	Water	Still in service

**New numbering system.

since the HRT achieved criticality. These operations have required an average of 36 man-hours for the removal and installation of the pump and 69 man-hours for removal and replacement of shielding blocks and seal pans.

The construction of ready-to-install units has cost an average of $5000 for feed pumps and $3000 for purge pumps.

6. SLURRY PUMPS

Diaphragm pumps appear to be adaptable to slurry, and tests with developmental pumps have been very encouraging.

6.1 Diaphragm Heads

It has been pointed out in Sec 3.2 that solids in the pump cavity may cause excessive diaphragm stresses by altering the diaphragm contour. There appear to be at least four possible solutions to the problem.

6.1.1 Maintenance. – Where maintenance is convenient and extreme longevity is not essential, the unit may be designed for ease of diaphragm replacement and the damage may be allowed to develop.

6.1.2 Filtration. – If the solids all exceed some conveniently filterable size, a reflux filter can be located in the pump head, in much the same way as the screens are located in solution pumps (cf. Sec 3.2), so that although the slurry passes through the head, the pump chamber operates only in clear liquid.

6.1.3 Remote-Leg Operation. – If the settling rate of the solids permits, the pump shown schematically in Fig. 33*a* will maintain a slurry-supernate interface in the vertical leg connecting the head and the check valves. The required length and diameter of the vertical leg depend on the settling rate of the slurry, the stroke volume and speed, and the necessary gas bleed and purge rates, if any. A test was conducted with 3-ft lengths of several different diameters of glass pipe for the vertical leg and with a slurry of water and 1600°C-fired ThO_2 (average particle size, 2 μ) having a specific gravity of 2. The test indicated that the average height of the interface above the check-valve intersection was a linear function of the average velocity in the vertical leg, going from 6 in. at a velocity of 1 in./sec to 28 in. at 11 in./sec. The dissolved gas in the slurry came out of solution at the reduced pressure of the suction stroke and traveled up into the pump head, carrying a coating of ThO_2 with it. This introduced some solids into the head and also necessitated a small, constant vent to prevent gas binding of the head. The venting created a net upward flow accompanied by a net rise of the interface in the vertical leg. The interface rise was offset by a small, constant purge of clear water introduced to the head on every suction stroke. With the vent and purge rates reasonably well balanced, the pump was satisfactorily operated at low discharge pressure for 1400 hr. When the head was disassembled, it contained some solids; however, the diaphragm showed very little evidence of damage. The head was reassembled as a high-pressure pump and has since

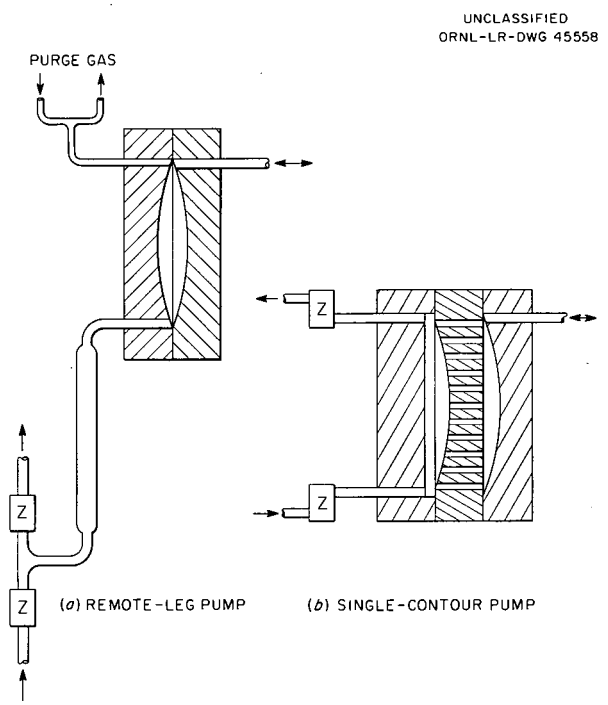

Fig. 33. (*a*) **Remote-Leg Pump;** (*b*) **Single-Contour Pump.**

pumped from 0.3 to 0.9 gpm of slurry at specific gravities of from 1.1 to 2.1 to discharge pressures of 500 to 1900 psi for 6200 hr. A continuous vent is used, but no purge is added. A sample point on the remote leg located 22 in. above the check valves yields samples of a specific gravity of 1.05, indicating that although a high degree of separation is achieved some solids are entering the head. Although this diaphragm did not fail, it was disassembled after 6200 hr and found to be quite heavily dented (see Fig. 34).

6.1.4 Single Contour. – Figure 33*b* illustrates a fourth adaptation, one that promises to give the longest service with the fewest problems. To eliminate the problem of solids between the diaphragm and the contour plate, the contour plate on the slurry side was eliminated and replaced by a simple recess. The diaphragm operates from the driving contour plate to center. This restricted motion is accomplished by coupling the pumping diaphragm in the left chamber to the driving diaphragm in the right chamber by the column of water between them. The driving diaphragm is restricted to stroking from the contour on its right to the flat face on its left. This arrangement permits the pump to take, in effect, only a half stroke, thereby reducing the capacity of the unit; however, the design considerably reduces the possibility of gas binding, since the pumped fluid is discharged out the top, and considerably reduces the possibility of diaphragm damage. A unit of this type pumped from 0.2 to 0.5 gpm of ThO_2 slurry for 6200 hr as a parallel unit to the remote-leg head (Sec 6.1.3). On disassembly the diaphragm was found to be completely unmarked (see Fig. 34). A duplex unit has been provided for engineering tests of an assembly of components proposed for slurry reactor use.

UNCLASSIFIED
PHOTO 34822

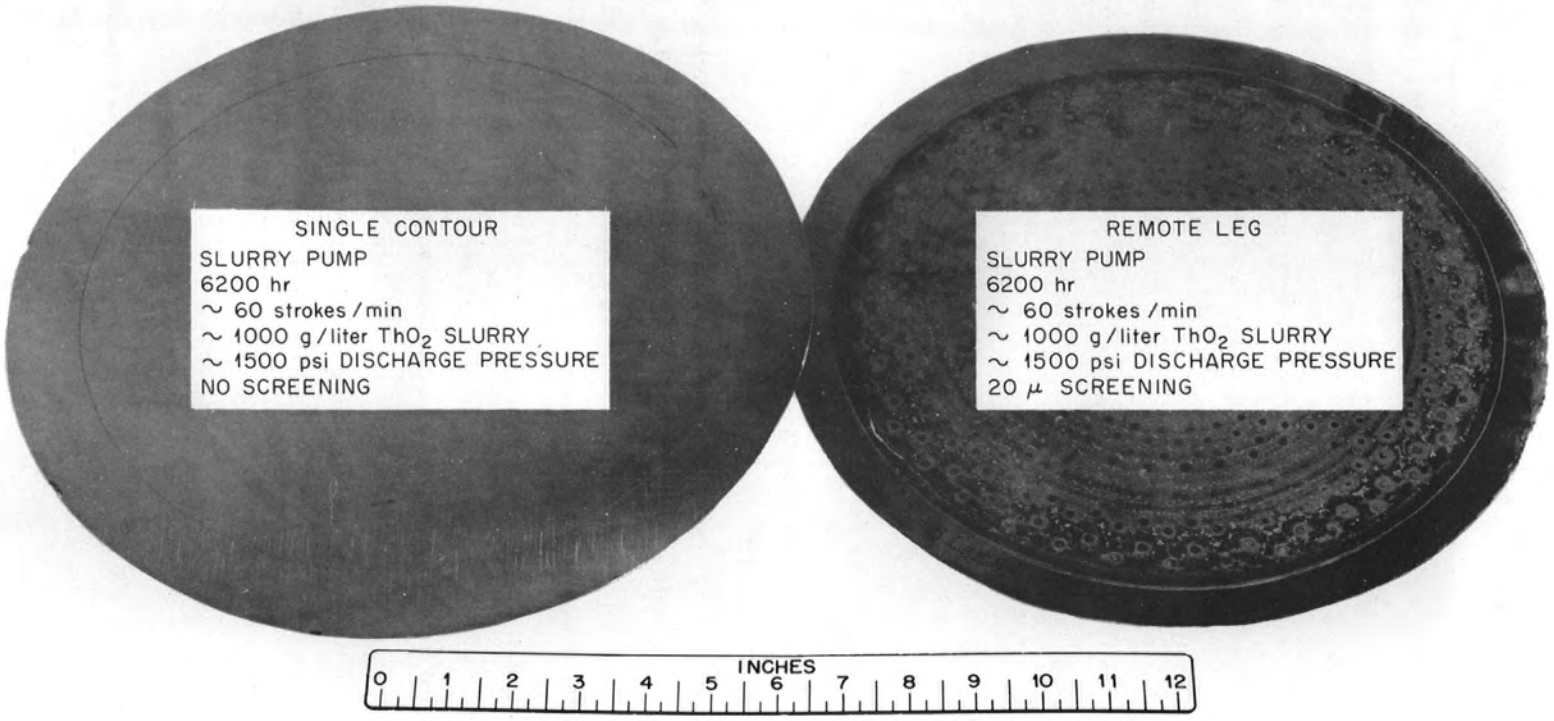

Fig. 34. Diaphragms from Single-Contour and Remote-Leg Slurry Pumps.

6.2 Check Valves

The problems of configuration and choice of structural materials are involved in the design of check valves for slurry service.

6.2.1 Configuration. – A slurry check valve should be designed for through flow with as few direction changes as possible. It should contain a minimum of horizontal surface to minimize deposition of solids, and the guiding of the ball should be in such a fashion that it cannot stick. Figure 32 is a double-ball dome-guided valve that has worked successfully in ThO_2 slurries of specific gravities up to 2.5.

6.2.2 Trim Material. – The trim material must be selected on the basis of experience under the conditions of intended use. Rubber and similar polymers have been successfully used industrially in abrasive slurries under some conditions. However, where a high-radiation environment exists, the choice is limited to metals, cermets, and ceramics. In the series of tests summarized in Table 8, the life of a trim material seemed to be related to its hardness. Thorium

Table 8. Tests of Check-Valve Trim

Average pump conditions:

Capacity, 0.5 gpm	Speed, 150 strokes/min
Suction pressure, atmospheric	Ball diameter, $\frac{5}{8}$ in.
Discharge pressure, 1500 psi	Configuration, single ball

Material, 1600°C-fired ThO_2 in water; specific gravity = 1.5 (~500 g/liter)

Trim Material		Hours of Operation	Results
Ball	Seat		
Al_2O_3	Zircaloy-2	2	Seats eroded
Al_2O_3	Gold	20	Seats badly eroded
Al_2O_3	Ti A-70	23	Seats badly eroded
17-4 PH	Ti A-70	19	Balls pitted; seats badly eroded
Stellite	347 SS	17	Balls pitted; seats badly eroded
Stellite	Stellite	99	Balls pitted; seats badly eroded
17-4 PH	17-4 PH	208	Seats eroded (192 hr of low-concentration slurry)
Tungsten carbide*	Tungsten carbide*	164	High leak rate
Al_2O_3	Al_2O_3	311	No flow loss; no static leakage; ball wear rate = 76 mpy
Al_2O_3	Al_2O_3	772	No flow loss; 1 cc/min leakage; ball wear = 45.6 mpy
Al_2O_3	B_4C	461	No flow loss; no static leakage; ball wear = 47.6 mpy
B_4C	B_4C	1550	No flow loss; balls slightly pitted; seat showed uniform wear; leak rates 25 cc/min discharge, 546 cc/min suction
Al_2O_3	BeO	1390	Indications of leakage after 200 hr; severe seat erosion

*Platinum bonded.

oxide is about 650 on the Knoop scale of hardness, or about equal to hardened steel at R_C 60.5. On the Knoop scale, BeO is 1220, ZrO_2 is 650, WC is 1880, Al_2O_3 is 2000, and B_4C is 2800. Scheduled for testing are ZrO_2, ThO_2, a variety of grades of Al_2O_3, and more B_4C.

It appears at this time that check valves capable of six months' continuous service in ThO_2 can be constructed. Since all materials tested suffer a finite wear rate, it is probable that planned replacement will be required, although continuous service is not called for in most of the proposed slurry applications.

7. DRIVE SYSTEMS

High-pressure diaphragm pumps must be hydraulically operated. Since the HRT feed pumps are exposed to radiation and since diaphragm rupture may introduce hydraulic fluid into the process fluid, the most acceptable hydraulic fluid is distilled water. The function of the drive system is to oscillate the operating column of water through a pressure cycle from suction pressure to discharge pressure and return with a volumetric amplitude sufficient to deflect the diaphragm the desired stroke. This can be accomplished directly by using a pulse generator that operates in water or indirectly by generating a pulse in oil and transferring it to the water column through an intermediate barrier. Although the direct water-pulse generator is attractive, since it eliminates the intermediate barrier and the necessity for obtaining and maintaining an exact amount of water in the closed column between the intermediate barrier and the pump diaphragm, the life of such generators tested to date has been short because of the poor lubricating properties of water. The added complexity of the oil-pulse generator system is more than offset by its long trouble-free life, and although the intermediate barrier required by the oil-pulse generator contributes to the complexity of the unit, it does provide an additional barrier against radioactive contamination of the pulse generator.

7.1 Pulse Generators

Two types of oil-pulse generators have been successfully used to drive reactor and experimental pumps.

The Scott and Williams P9 slide-valve pulse generator, used to drive the HRT feed pumps, consists of a rotary positive-displacement oil pump discharging into a slide-valve distributor that lets oil into and out of each of two intermediate expandable barriers (the pulsator of Fig. 1). The energy for the suction stroke of the pump is provided by stored energy in the expanded intermediate barrier. The variable-delivery oil pump permits variation of pulse volume while stroking speed remains constant. The time-displacement curve of the slide-valve unit is virtually a square wave, leading to high accelerations at the beginning and end of each stroke. In early designs, the columns of liquid in the suction and discharge lines plus the closed columns in the drive lines set up moderate to severe oscillations or water hammer in response to the accelerations. This hammer was evidenced by noise, vibration, pressure oscillations of several

hundred pounds, check-valve chatter, and diaphragm flutter. Altering the spool piece[10] by adding tapered intake and exhaust portions (Fig. 35) decreased the accelerations and considerably reduced the accompanying hammer (Fig. 36). This modification was made to the HRT drive units, which have operated satisfactorily and required little maintenance. A relief valve in the high-pressure oil system limits the pressure in the entire pump system in the event of overphasing (see Sec 7.3) or of any line plugging. The relief valve is usually set about 10% above pump discharge pressure.

The reciprocating pulse generator, used to drive the HRT purge pumps and some experimental pumps, consists of a plunger in a cylinder with a radial port arranged so that the plunger uncovers the port at the end of each suction stroke. The cylinder operates submerged in oil,

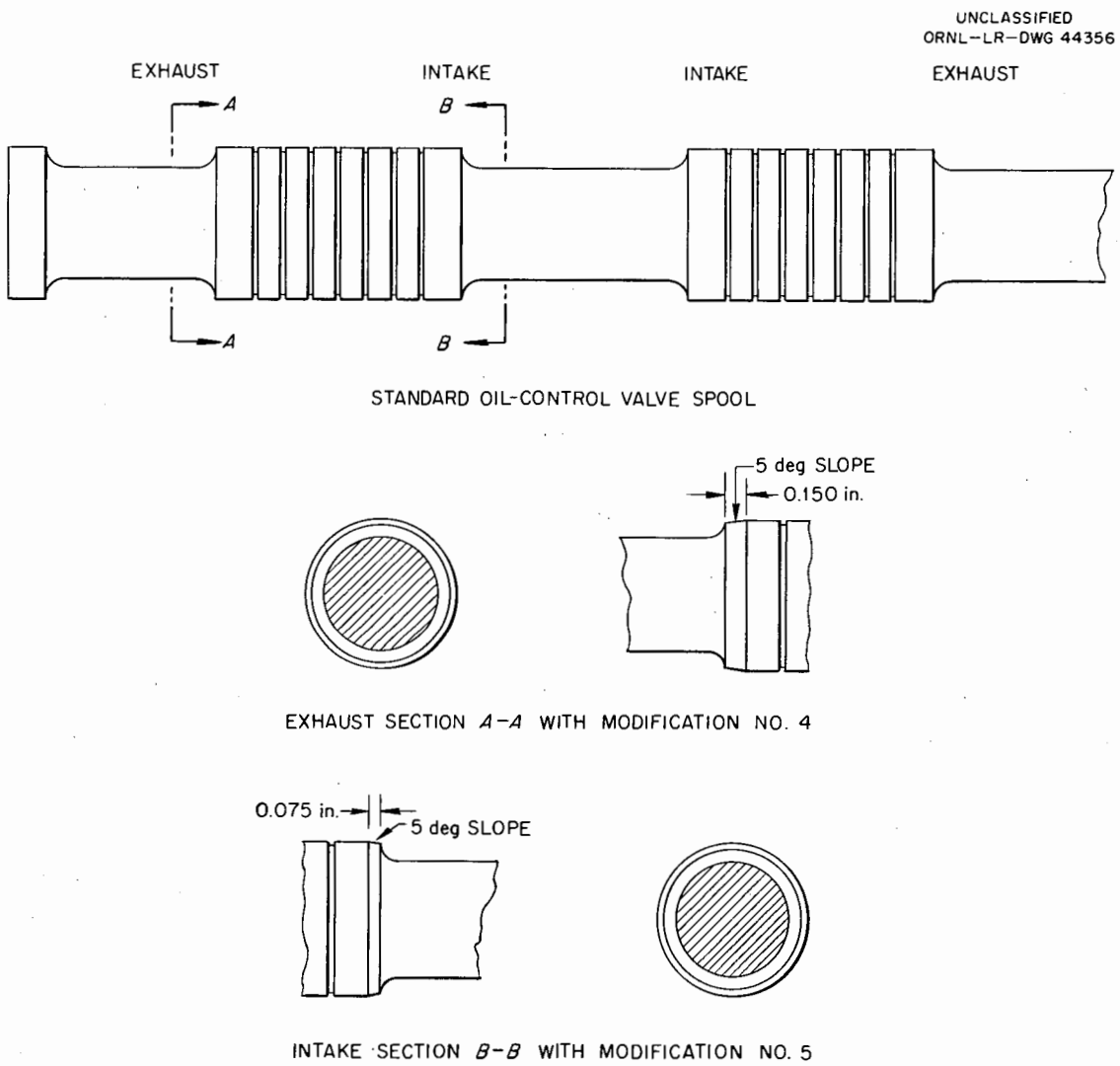

Fig. 35. Oil-Control Slide-Valve Spool.

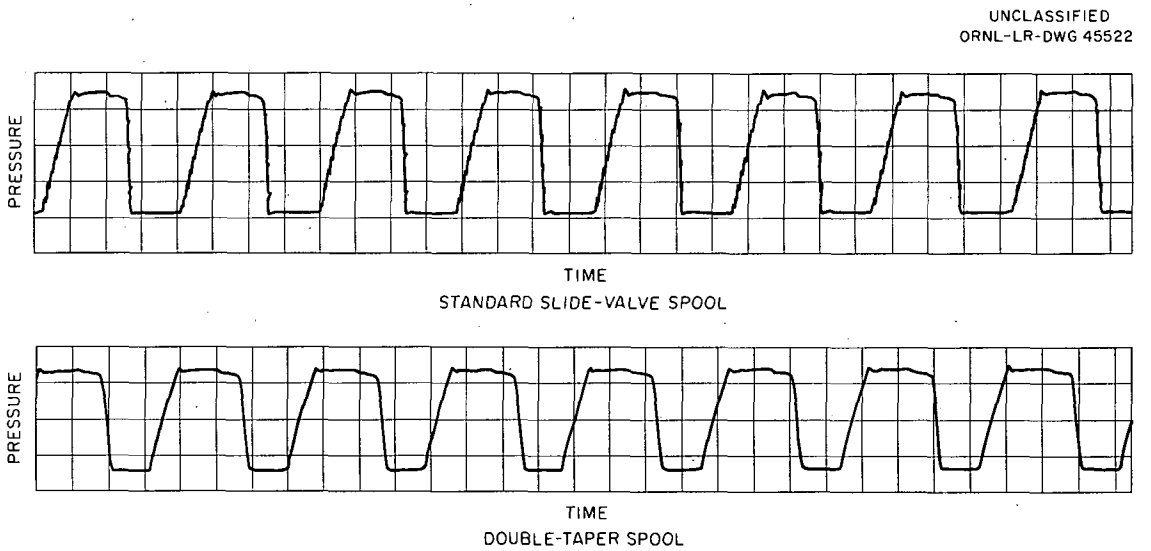

Fig. 36. Pressure vs Time Traces from an HRT Feed Pump with a Scott and Williams Drive.

permitting the port to make up plunger leakage on each stroke; thus the plunger and the intermediate barrier start their effective stroke at the same point in each cycle. The reciprocating drive provides the energy for the diaphragm suction stroke, creating somewhat more favorable suction conditions. Since the time-displacement curve of the reciprocating drive is sinusoidal, or nearly so, the system operates very quietly and smoothly.

The Scott and Williams 1 LB reciprocating pulse generator is used to drive the HRT purge pumps. Milton Roy simplex and duplex and John Bean triplex power ends have been fitted with pulse cylinders to drive experimental pumps. Reciprocating pulse generators should be protected by a relief valve in a fashion similar to that for the slide-valve pulse generator.

Units of the slide-valve type are available with capacities up to 242 gpm, and other capacities can be created by using appropriately sized commercially available oil pumps and slide valves. Reciprocating pulse generators are available in sizes up to 1 in.^{3} per stroke; other sizes can be made by fitting a suitable commercially available simplex, duplex, or triplex power end with a plunger and ported barrel of the appropriate size. In either case the required pulse volume can be approximated from

$$V_p = V_s + \frac{PV_D}{2 \times 10^5} ,$$

where

V_p = pulse volume, in.^{3},

V_s = desired volumetric stroke of the diaphragm head, in.^{3},

P = discharge pressure, psi,

V_D = fluid volume of the hydraulic drive system (both oil and water if a two-fluid system is used), in.^{3}.

The term $PV_D/2 \times 10^5$ represents the pressure-cycle losses in the hydraulic drive system which, in the HRT feed pump, are about equal to the desired volumetric stroke of the diaphragm head, so that the capacity of the drive unit must be twice the desired capacity of the feed pumps. Figure 37 shows a comparison of the calculated individual fluid compressibility and system expansion volumes, the measured over-all ΔV required to obtain a 2000-psi ΔP in the drive system under static conditions, and the difference between pulse volume and pump output under dynamic conditions for a pump system similar to that of the HRT.

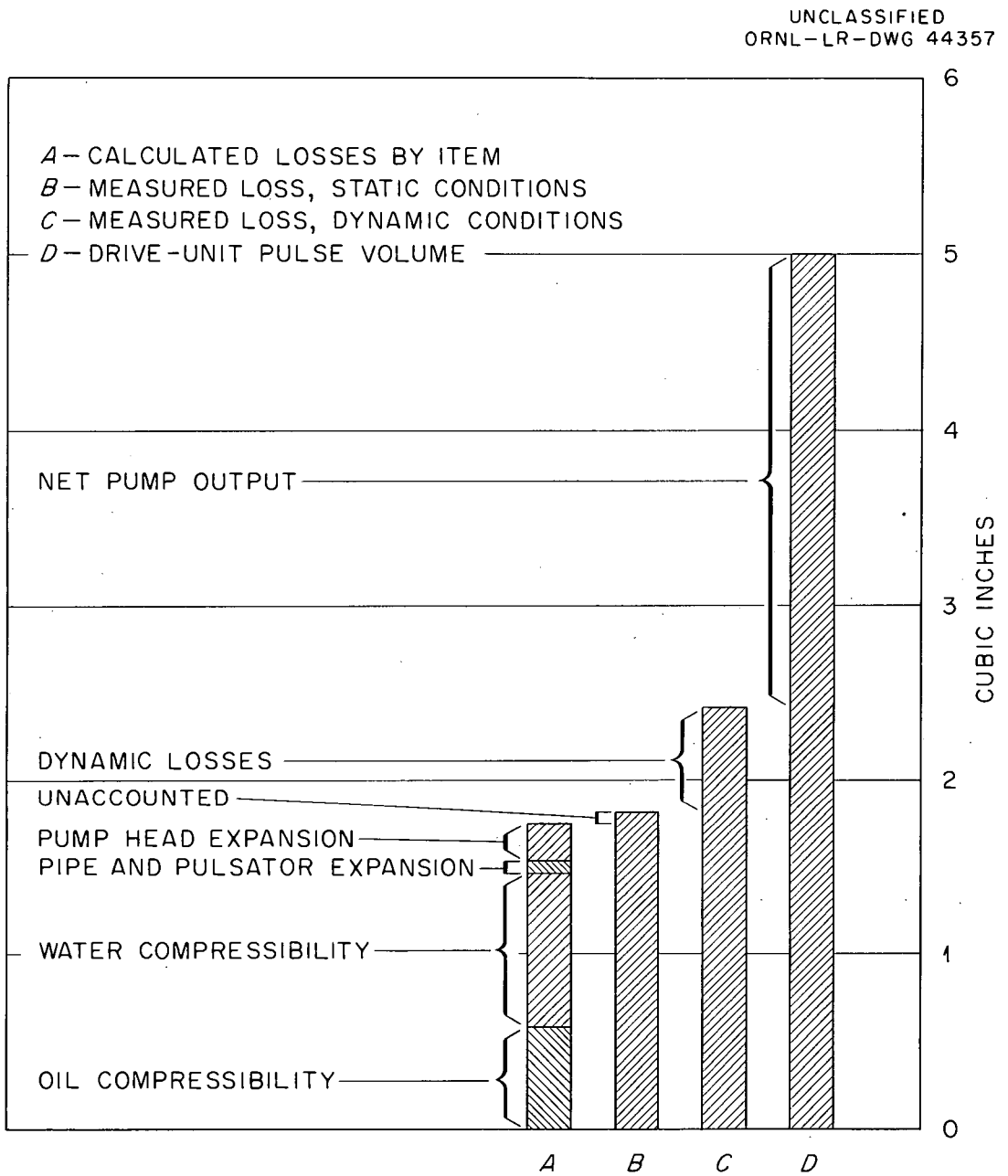

Fig. 37. Volumetric Losses per Stroke in a Two-Fluid Drive System with Intermediate Barrier; V_D = 170 in.^{3}.

Having determined the required pulse volume, V_p, and the discharge pressure, the appropriate pulse generator can be selected.

7.2 Intermediate Barriers

Intermediate barriers are used to transmit the pulse from oil to water and to separate the two systems. Since the barrier can be located outside the radiation field, a wide choice of materials is available. The Scott and Williams pulsator (Fig. 1) currently in use consists of a perforated hollow steel mandrel, two nested rubber boots fitted over the mandrel, and a forged stainless steel pressure chamber. As oil is alternately introduced and exhausted through the mandrel, the rubber boots expand and contract, forcing water out of and into the pressure housing and transmitting the pulse through the isolation pipe to the diaphragm head. A leak detector monitors the space between the two boots and automatically shuts off the pulse generator if either boot ruptures. The forged pressure chambers have suffered no failures, and with proper usage the boots have a life in excess of 5000 hr. The Scott and Williams intermediate barrier is available in maximum stroke volumes of 0.55, 1.00, 5.00, 14.50, and 168.0 in.^{3}.

7.3 Phasing of Intermediate Systems

The volume of water from the intermediate barrier through the isolation drive line to the pump diaphragm is referred to as the intermediate system. The operation of obtaining the correct volume of water in the intermediate system is referred to as phasing. Insufficient water will allow the pump diaphragm to bottom on the driving contour plate before the end of the suction stroke. Too much water will cause it to bottom on the pumping contour plate before the end of the discharge stroke. Either condition reduces the output of the pump and creates undesirable operating characteristics.

The allowable latitude in phasing is dependent upon the ratio of actual stroke volume to available stroke volume and upon the type of drive system used. The HRT fuel-pump heads have an available diaphragm stroke of 6.5 in.^{3}, but the output is limited by the drive to 2.5 in.^{3}. With the Scott and Williams P9 drive unit used, the rubber boot must provide the pressure differential to deflect the diaphragm on the suction stroke, and therefore it does not return completely to the mandrel. The degree to which the boot floats off the mandrel will depend on the degree to which the diaphragm is pulled in toward the contour plate on the water side at the end of the suction stroke. This pump will appear to be in correct phase through a variation of about 6 in.^{3} of water in the intermediate system. With a diaphragm head that is using all or most of its displacement and is driven by a reciprocating drive that can seat the boot firmly on the mandrel at the end of each suction stroke, the latitude is reduced to a fraction of a cubic inch.

With the Scott and Williams P9 drive, the correct phasing for any set of suction and discharge conditions must be determined experimentally. This is best accomplished, while watching a pressure vs time trace of the intermediate system, by adding water with the phasing

system illustrated in Fig. 1 until the system becomes overphased (Fig. 38*b*) and then removing water until the overphase indication disappears (Fig. 38*a*). If at the time of phasing the discharge pressure is insufficient to register on the pressure trace, then a pressure rise above the base line is an overphase indication. For the reciprocating drive, a predetermined phasing can be used regardless of the conditions. This is accomplished by filling the intermediate system in such a fashion that the rubber boot is seated on the mandrel and the diaphragm is deflected against the process-side contour plate, and then removing a quantity of water equal to the stroke of the diaphragm. In either case the phasing operation is simple and straightforward.

ACKNOWLEDGMENT

The author is especially indebted to R. N. Lyon of the Reactor Experimental Engineering Division for his careful review of this report and for his many helpful suggestions during its preparations.

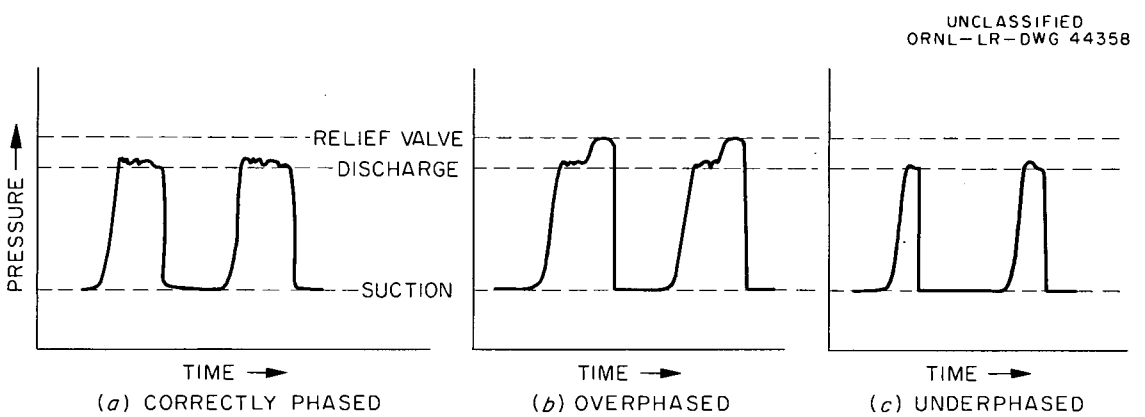

Fig. 38. Pressure vs Time Traces for Various Conditions of Phasing.

ORNL-2841
UC-38 – Equipment, Methods, and Techniques
TID-4500 (15th ed.)

INTERNAL DISTRIBUTION

1. HRP Director's Office
2. S. E. Beall
3. A. M. Billings
4. D. S. Billington
5. R. Blumberg
6. E. G. Bohlmann
7. S. E. Bolt
8. J. R. Brown
9. W. D. Burch
10. C. E. Center
11. R. H. Chapman
12. R. A. Charpie
13. R. S. Cockreham
14. E. L. Compere
15. F. L. Culler
16. D. G. Davis
17. R. J. Davis
18. O. C. Dean
19. D. M. Eissenberg
20. L. B. Emlet (K-25)
21. J. L. English
22. D. E. Ferguson
23. C. H. Gabbard
24. W. R. Gall
25. J. P. Gill
26. R. S. Greeley
27. J. C. Griess
28. W. R. Grimes
29. P. A. Haas
30. P. H. Harley
31. C. S. Harrill
32. P. N. Haubenreich
33. J. W. Hill
34. E. C. Hise
35. H. W. Hoffman
36. A. Hollaender
37. G. H. Jenks
38. W. H. Jordan
39. P. R. Kasten
40. G. W. Keilholtz
41. C. P. Keim
42. M. T. Kelley
43. M. J. Kelly
44. J. A. Lane
45. C. G. Lawson
46. S. C. Lind
47. R. S. Livingston
48. R. A. Lorenz
49. M. I. Lundin
50. R. N. Lyon
51. W. L. Marshall
52. J. P. McBride
53. H. F. McDuffie
54. R. E. Moore
55. R. L. Moore
56. C. S. Morgan
57. K. Z. Morgan
58. J. C. Moyers
59. J. P. Murray (Y-12)
60. M. L. Nelson
61. L. F. Parsly, Jr.
62. H. R. Payne
63. F. N. Peebles
64. D. Phillips
65. M. L. Picklesimer
66. J. L. Redford
67. S. A. Reed
68. W. D. Reel
69. P. M. Reyling
70. D. M. Richardson
71. R. C. Robertson
72. M. W. Rosenthal
73. H. C. Savage
74. D. Scott, Jr.
75. C. H. Secoy
76. E. D. Shipley
77. M. D. Silverman
78. M. J. Skinner
79. A. H. Snell
80. I. Spiewak
81. J. A. Swartout
82. A. Taboada
83. E. H. Taylor
84. D. G. Thomas
85. M. Tobias
86. W. E. Unger
87. G. M. Watson
88. A. M. Weinberg
89. G. C. Williams
90. C. E. Winters

91–92. Reactor Experimental Engineering Library
93–94. Central Research Library
95–114. Laboratory Records Department
115. Laboratory Records, ORNL R.C.
116–117. ORNL – Y-12 Technical Library, Document Reference Section

EXTERNAL DISTRIBUTION

118. D. H. Groelsema, AEC, Washington
119. Division of Research and Development, AEC, ORO
120. L. Weller, Mound Laboratory, Miamisburg, Ohio
121–576. Given distribution as shown in TID-4500 (15th ed.) under Equipment, Methods, and Techniques category (75 copies – OTS)